

# Photoluminescence in Mercury Cadmium Telluride – a Historical Retrospective. Part II: 2004–2022

M.S. Ruzhevich<sup>1</sup>, K.D. Mynbaev<sup>1,2,\*</sup>

<sup>1</sup> Institute of Advanced Data Transfer Systems, ITMO University, Kronverkskiy pr., 49, lit. A, Saint-Petersburg 197101, Russia

<sup>2</sup> Department of Solid-State Physics, Ioffe Institute, Politekhnikeskaya ul., 26, Saint-Petersburg 194021, Russia

---

## Article history

Received December 10, 2022

Received in revised form

December 20, 2022

Accepted December 23, 2022

Available online December 30, 2022

## Abstract

This review is a second part of the work that presents a historical retrospective of the studies of photoluminescence in mercury cadmium telluride (HgCdTe), one of the most important materials of infrared photo-electronics. The second part of the review considers the results of the studies performed in 2004–2022. These studies were carried out mostly on films grown by molecular beam epitaxy and focused on the investigation of defects, especially those originating in *p*-type doping with mercury vacancies or arsenic atoms. Compositional uniformity and alloy fluctuations in HgCdTe were also the subjects of the studies.

---

**Keywords:** HgCdTe; Luminescence; Defects; Composition fluctuations

This review considers the results of the study of photoluminescence (PL) in mercury cadmium telluride (MCT, HgCdTe) performed in 2004–2022. The authors should like to dedicate the review to the memory of Prof. V.I. Ivanov-Omskii (1932–2022), who was one of the pioneers of MCT technology and research. Obituary to Prof. V.I. Ivanov-Omskii (in Russian) can be found in *Fizika i Tekhnika Poluprovodnikov*, 2022, vol. 56, no. 10, pp. 1016–1017. Prof. Ivanov-Omskii published his first paper on optical properties of MCT back in 1964 [1] and devoted 55 years of his life to the synthesis and study of various properties of this material, especially optical and photoelectrical properties, which was duly appreciated by the MCT community (see, e.g., Ref. [2]).

This work is a second part of the general review, where the first part was related to some of the general properties of MCT and to the results of PL studies performed in 1966–1996 [3]. As mentioned in Ref. [3], with MCT being strongly demanded in defense applications, its science and technology experienced a boom during the cold war era, and by the mid-1990s the interest in this material was not so strong. At that point, it was also

believed that MCT-based photodetectors would be soon replaced by detectors based on III-V materials. As a result, the number of research papers devoted to the studies of MCT in the late 1990s was decreasing, and to the best of the knowledge of the authors of this review, no papers on PL in MCT were published between 1996 and 2004. By the mid-2000s, however, it became obvious that ultimate performance infrared (IR) photodetectors made of MCT will remain superior to their III-V counterparts at least for some years [4], and the interest in MCT resumed with the number of research papers steadily growing. PL studies of MCT were no exception, so the second part of the review will consider works on PL in MCT published since 2004, when the ‘new era’ of PL studies of MCT began. In this part of the review we shall again concentrate on optically pumped spontaneous emission from ‘bulk’ MCT samples; this time, these will be epitaxial films and heteroepitaxial structures with no size quantization effects. Nanostructures, including superlattices, and quantum-well (QW) structures, and laser action in MCT will not be considered. The material under consideration in this part of the review would be mostly grown by Liquid Phase

---

\* Corresponding author: K.D. Mynbaev, e-mail: [mynkad@mail.ioffe.ru](mailto:mynkad@mail.ioffe.ru)

Epitaxy (LPE) on lattice-matched CdTe or ZnCdTe substrates and by Molecular Beam Epitaxy (MBE) or Metalorganic Chemical Vapor Deposition (MOCVD) on ZnCdTe substrates or ‘alternative’ substrates made of Si or GaAs.

Many of the studies performed in the last 20 years were devoted not to the investigation of PL in MCT as such, but to the study of various defects in MBE-grown material, and in particular, defects formed in *p*-type MCT doped with mercury vacancies or/and arsenic. Acceptor doping of MCT has been an issue for a number of years [5,6]. Historically, mercury vacancy  $V_{\text{Hg}}$  was regarded as an easily available and suitable acceptor, and the vacancy doping has been used in fabrication of MCT-based *p-n* junctions for many years. It appeared, however, that this doping produced not only shallow, but also deep levels in the bandgap, and the latter acted detrimentally on the properties of photodetectors [7–9]. Also, the exact energy spectrum of vacancy-related levels in MCT remains a subject of discussion [10,11] as well as the effect of vacancy doping on the absorption edge and the cut-off wavelength of photodetectors [12]. As to the extrinsic doping, with the advent of MBE-grown heterostructures comprising very thin layers, traditional acceptor impurities for MCT, such as Au, Ag or Cu had to be abandoned due to their fast diffusivity related to the interstitial mechanism of propagation [6]. Arsenic has low diffusivity and has been always considered to be a shallow acceptor. A problem related to arsenic doping of MCT is caused by the manner of its incorporation, as as-grown MBE films doped with arsenic typically show *n*-type conductivity. Originally, it was suggested that the reason for that was the amphoteric nature of arsenic that could occupy both cation sites as a donor  $\text{As}_{\text{Hg}}$  and tellurium sites as an acceptor  $\text{As}_{\text{Te}}$  [5,6]. Later, more complicated mechanisms of arsenic incorporation and activation in MCT were proposed, which will be discussed in some detail below. In any case, under typical MBE conditions (enrichment with tellurium), arsenic is generally incorporated in MCT as a donor, and a post-growth activation of the arsenic acceptor is necessary to achieve *p*-type conductivity. This activation is usually performed via a two-step annealing, which includes ‘arsenic activation’ (AA, e.g., annealing at  $\sim 400$  °C for 1 h) and ‘vacancy filling’ (VF, annealing in saturated mercury vapors, e.g., at  $\sim 200$  °C for  $\sim 24$  h) steps. AA annealing produces arsenic acceptors, while VF annealing reduces concentration of mercury vacancies  $V_{\text{Hg}}$  which are generated during the AA stage. At that, activation induces not only  $V_{\text{Hg}}$ , but also other defects that may affect the properties of the material, and that makes studies of defects in arsenic-doped MCT quite a topical task.

The number of research groups that have performed PL studies in MCT in the last 20 years was not large; these

groups were located mostly in France, China and Russia. Let us start with the PL studies that were performed in France; these relate to 2009–2014 time span.

One of the first modern works of French scientists from Département Optronique at LETI, CEA on PL in MCT was the 2009 journal paper by Robin *et al.* [13]. It was devoted to the study of  $\text{Hg}_{1-x}\text{Cd}_x\text{Te}$  films with  $x = 0.3$  grown by MBE on ZnCdTe substrates and doped with arsenic. To this end, modulated PL measurements with a continuous-scan Fourier transform infrared (FTIR) spectrometer were performed using a 1064 nm Nd:YAG laser for excitation. Three peaks were observed in the spectra both for as-grown and annealed samples. The high energy (HE) peak located at 245 meV was assigned to interband transitions; this peak did not shift after the annealing. Robin *et al.* [13] believed that the low-energy (LE) and mid-energy (ME) peaks (located at 239 and 230.2 meV in as-grown films, respectively) had a different nature in the sample before and after the annealing. Namely, in the as-grown film the LE peak was attributed to the presence of  $V_{\text{Hg}}$ , while after VF annealing, to the  $\text{AsHg}$  complex, which was also an acceptor. The ME peak in the as-grown film was attributed to the  $\text{As}_2\text{Te}_3$  donor complex, and so was the case of the sample after the VF annealing. After the AA+VF annealings, the nature of this peak was explained by the presence of  $\text{As}_{\text{Hg}}$ .

These ideas were further developed in conference papers [14,15], where in addition to arsenic-doped films, undoped and indium-doped samples were studied. The PL spectrum of the undoped sample with  $x = 0.32$  contained one peak at 266 meV; after VF annealing, a second peak appeared at low temperatures at 260 meV. The latter was attributed to either a band-to-level transition or donor-acceptor-pair (DAP) transitions. The behavior of the main peak was similar before and after ‘*p*-type’ (PT, generating mercury vacancies at 330 °C for 1 h in vacuum) annealing: at low temperatures ( $2 < T < 160$  K), the peak energy was smaller than the value of the bandgap  $E_g$ , and as the temperature increased over 160 K, the energy of the peak approached the bandgap (Fig. 1, the formula for bandgap calculations was not specified by Robin *et al.*). This behavior was explained by carrier localization in the tails of the Urbach states due to composition fluctuations of the solid solution. The PL spectrum of the as-grown indium-doped sample with  $x = 0.45$  contained two peaks with energies of 499 meV and 513 meV, respectively. After VF annealing, the intensity of the HE peak strongly decreased, 499 meV peak disappeared, emission at 492 meV was detected, and a broad band at 400 meV also appeared. The latter was attributed to DAP emission, probably involving transitions between indium donor levels and deep acceptors. The temperature-driven behavior of the HE peak repeated the temperature dependence of the energy of PL peak  $E_{\text{PL}}$  for the undoped sample, showing at  $T < 120$  K

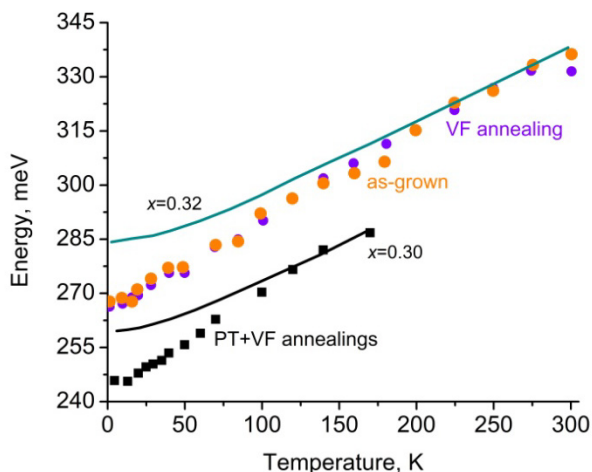


**Fig. 1.** Temperature dependences of HE PL peak energy (symbols) vs calculated  $E_g(T)$  (solid lines) for MBE-grown films with  $x = 0.30$  [13] and  $x = 0.32$  [15].

localization in the tails of the Urbach states (Fig. 1). This peak certainly corresponded to interband transitions, while the LE peak (499 meV) before annealing was associated with transitions to  $V_{\text{Hg}}$  acceptors, and after annealing (492 meV), to DAP transitions between indium donor levels and deep acceptors, as mentioned above. Robin *et al.* concluded in Refs. [14,15] that the studies on the indium-doped sample showed that VF annealing both activated impurities and reduced alloy non-uniformity.

The PL spectra of the sample doped with arsenic discussed in Refs. [14,15] had been described by Robin *et al.* in Ref. [13] (see above). On the basis of these results, ionization energies of various donors and acceptors were calculated. In particular, the ionization energy of the  $V_{\text{Hg}}$  acceptor appeared to be 15 meV (Fig. 2a), and that of the  $\text{AsHg}$  acceptor complex was found to be 12.8 meV. The ionization energy of the  $\text{As}_2\text{Te}_3$  donor complex was estimated to be 5.5 meV, and that of the  $\text{AsHg}$  donor was 7.8 meV.

The studies related to optical signatures of  $V_{\text{Hg}}$  were continued by Gemain *et al.* [10,16]. To this end, the PL spectra of LPE-grown samples with  $x = 0.327$  before annealing and after VF and PT annealings were compared. The PL spectrum of the as-grown sample contained three peaks with  $E_{\text{PL}}$  of 234.5 meV (LE), 251.1 meV (ME), and 261.8 meV (HE). The HE peaks was attributed to interband transitions, as was confirmed by the variable-temperature PL measurements. Two other peaks disappeared from the PL spectrum after VF annealing and began to dominate after PT annealing. These peaks ceased to be visible at  $T > 150$  K due to the ionization of acceptor levels to which the optical transitions from the conduction band CB ( $c$ - $A$ ) occurred. It was concluded that these peaks belonged to the transitions to the two acceptor levels of mercury vacancies, associated with their ionized

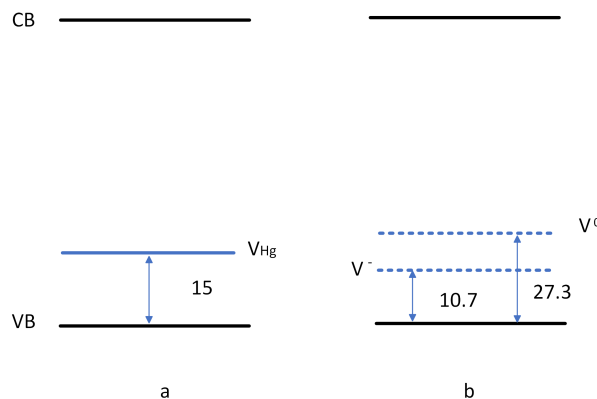


**Fig. 2.** Mercury vacancy state(s) energy ordering in MCT according to Robin *et al.* [13] (a) and Gemain *et al.* [16] (b). Values are given in meV.

states  $V^-$  and neutral states  $V^0$ . Gemain *et al.* [10,16] calculated two ionization energies of  $V_{\text{Hg}}$  in undoped MCT as 10.7 meV and 27.3 meV, and to identify the states, they employed the Hall-effect data. Only one activation energy (26.2 meV) was found in the temperature-dependent Hall-effect measurements, which suggested, according to Gemain *et al.* [10,16], that the mercury vacancy in MCT is a ‘negative-U’ defect with the ionized state having 10.7 meV energy and the neutral state of 27.3 meV (Fig. 2b). Note that a relatively deep level ( $\sim 25$  meV from either the bottom of the CB or the top of the valence band VB) was also found in PL decay studies of vacancy-doped MCT with  $x \approx 0.3$  by Delacourt *et al.* [7]. Gemain *et al.* [17] established, again with the use of both PL and the Hall-effect measurements performed on LPE-grown samples, that with an increase in the  $x$  value from 0.32 to 0.6 these two ionization energies increased to 18 meV and 38 meV, respectively. According to Gemain *et al.* [17], this meant that with the increase in the  $x$  value, the Jahn-Teller effect responsible for the negative-U property of  $V_{\text{Hg}}$  for low  $x$  became overpassed by the Coulomb repulsion. This was explained by a decrease of the dielectric constant with the increase in  $x$ , which led to an enforcement of the Coulomb repulsion.

Arsenic-related studies were continued by Gemain *et al.* in Ref. [18]. These studies (again, accompanied with the Hall-effect measurements) were meant to confirm the findings obtained with Extended X-Ray Absorption Fine Structure (EXAFS) measurements carried out by Ballet *et al.* [19] and Biquard *et al.* [20]. The findings seemingly contradicted the widely accepted models by Berding and Sher [21] and Vydyanath [22], which implied that during MBE under tellurium-rich conditions arsenic is incorporated as an  $\text{AsHg}$  donor and that the high temperature annealing, i.e., AA annealing, just transfers arsenic atoms from mercury sublattice into tellurium one, so they become  $\text{As}_{\text{Te}}$  acceptors. Ballet *et al.* [19] and

Biquard *et al.* [20] suggested that before AA annealing, arsenic atoms are approximately equally shared between a donor structure locally resembling the chalcogenide glass  $\text{As}_2\text{Te}_3$  and an acceptor structure  $\text{AsHg}_8$  consisting of an As atom surrounded by 8 Hg nearest-neighbor atoms in a locally body-centered cubic structure. According to Ballet *et al.* [19] and Biquard *et al.* [20], after AA annealing, the  $\text{As}_2\text{Te}_3$ -like donor gets dissociated. Approximately 2/3 of the arsenic atoms get incorporated as  $\text{AsHg}_8$  acceptors and 1/3 is incorporated as  $\text{AsHg}$ , so the concentration of arsenic-related acceptors is higher than that of arsenic-related donors, and  $p$ -type conductivity is observed, with some electrical compensation. In Ref. [18], Gemain *et al.* found activation energies for these acceptor and donor complexes from low-temperature PL measurements and temperature-variable Hall measurements performed on MBE-grown sample with  $x = 0.31$ . Ionization energy of 15.2 meV was found for an  $\text{As}_2\text{Te}_3$ -like donor, 11.8 meV for an  $\text{AsHg}$  donor, and 26.8 meV for an  $\text{AsHg}_8$  acceptor. Interestingly, activation energy for an arsenic acceptor of 31.5 meV was found as early as in 1996 by the Chinese researchers [23]. Guo *et al.* [23] studied arsenic-implanted and activated MBE-grown sample with  $x = 0.39$ , so their result would be in line with the idea of the increase in the arsenic acceptor activation energy with increase in the  $x$  value established by Gemain *et al.* in Ref. [17]. Guo *et al.* [23], though, believed that they detected optical signature of the  $\text{AsTe}$  acceptor, not  $\text{AsHg}_8$ , the latter having not been discovered yet at the time.

Summarizing the PL studies of the French researchers, it should be noted that they were performed not just on their own but with the conjunction with other methods, such as EXAFS and the Hall-effect measurements. These comprehensive studies produced interesting new results, such as the hypothesis on the negative-U properties of  $\text{V}_{\text{Hg}}$  and new mechanism of arsenic incorporation and thermal activation in MBE-grown MCT.

The works by the researchers from the Shanghai Institute of Technical Physics such as mentioned here Ref. [23] continued, and in 2006, a new technique for optical studies of narrow-bandgap MCT was presented. The technique was based on photo-modulated spectroscopy using a step-scan FTIR spectrometer [24]. Photo-reflectance (PR) spectra recorded in 5 to 9  $\mu\text{m}$  wavelength range were compared to PL spectra. Arsenic-doped MBE-grown film with  $x = 0.313$  and undoped LPE-grown film with  $x = 0.235$  were used in the study performed at  $T = 77$  K. In both cases, the PL spectra contained only one peak which was interpreted as fundamental-bandgap-related one. The advantages of the new PL registration technique in respect to signal-to-noise ratio, etc., were further demonstrated by Shao *et al.* for MBE-grown films with  $x = 0.52$  and

$x = 0.30$  [25]. In these experiments, the measurements were performed using a Bruker IFS 66 v/S FTIR spectrometer with PL excitation by a mechanically chopped (1.8-kHz) focused 514.5 nm line of an argon laser.

Modulated PL spectroscopy with a step-scan FTIR spectrometer was used for the study of the so-called blue-shift in PL and photoconductivity (PC) spectra of the  $n$ -on- $p$  MCT photodiodes fabricated with ion milling [26,27]. Ion milling or ion (plasma) etching are used in MCT technology for fabrication of  $n$ -on- $p$  photodiode structures, as low-energy (1 to 5 keV) ion or plasma treatment causes controllable  $p$ -to- $n$  conductivity type conversion in  $p$ -type material [28,29]. Zha *et al.* [26,27] reported that a sequence of PL spectra measured across a square  $p$ - $n$  junction fabricated with ion milling showed luminescence peaks of the milled area shifting strongly to shorter wavelengths in comparison to the spectra of the initial LPE-grown  $p$ -type material. This blue-shift could not be attributed to the composition non-uniformity of the material, as the value of the shift was  $\sim 39$  meV and was much larger than the non-uniformity-related energy uncertainty of  $\sim 6$  meV as revealed by PL measurements performed at different spots of the sample. The shift was interpreted in terms of Burstein-Moss (BM) effect, as electron concentration in the milled area (assessed as  $n \approx 7.2 \times 10^{16} \text{ cm}^{-3}$ ), according to Zha *et al.* [27], exceeded threshold concentration of  $n$ -region for the occurrence of the effect (which was estimated to be  $n \approx 8 \times 10^{15} \text{ cm}^{-3}$  for  $T = 77$  K and  $E_g = 0.197$  eV). To explain the exact value of the shift, it was noted that a red-shift of the absorption peak was previously found for  $p$ -type MCT with  $\text{V}_{\text{Hg}}$  acting as acceptors [30]. The value of this shift was 9–12 meV from the bandgap edge in the temperature range of 30–70 K. The shift was explained by the mixing of the thermal activation energies of the VB and the vacancy acceptor levels. The PL spectrum of the  $n$ -on- $p$  diode fabricated with ion milling contained two peaks. One was from the  $p$ -type region and its energy was  $\sim 10$  meV smaller than the calculated bandgap value due to the high concentration of  $\text{V}_{\text{Hg}}$ . The second peak from the  $n$ -type region was shifted by 39 meV towards higher energies, which was expected since the vacancies were filled during the milling. However, vacancy filling should have shifted the peak just by the above mentioned 10 meV, which was much less than the actual shift. Therefore, the rest of the shift (29 meV) was attributed to the BM effect, with calculations of the Fermi level shift as a result of heavy electron doping confirming its exact value. The authors of this review would like to note, though, that the shift observed by Zha *et al.* [26,27] should not be, in fact, permanent, as electron concentration in ion-milling-induced  $n$ -type material is prone to relaxation and gradually decreases with time [29,31].

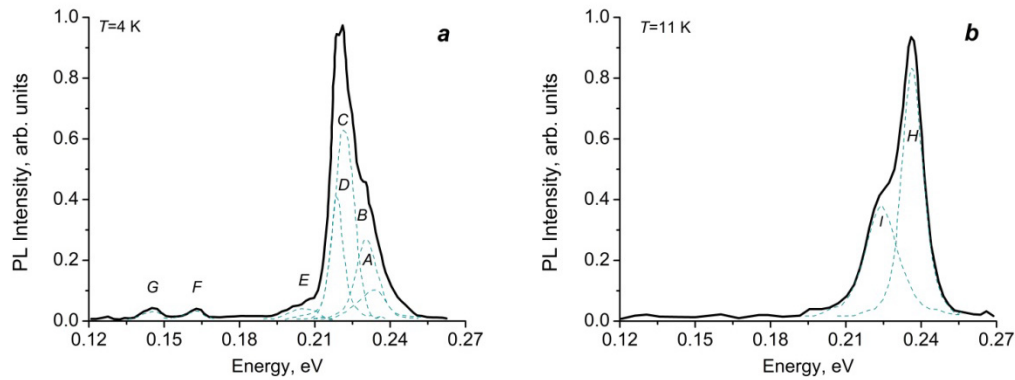


**Fig. 3.** PL spectra of as-grown (a) and annealed (AA+VF annealings) (b) MCT film with  $x = 0.298$ . Solid lines show experimental data, dashed lines show spectra deconvolution (replotted using the data from Ref. [36]).

Using both the Hall-effect and PL measurements, Pociask *et al.* [32] showed that the electron concentration in the milled material indeed decreases, and after the relaxation, whose characteristic time depends on the parameters of the material (e.g. the  $x$  value) goes below the BM threshold, so for the ‘relaxed’ samples no blue-shift of the PL band should be observed. In particular, in relation to the PL spectra, a consecutive red-shift of the peak was observed by Pociask *et al.* [32] for those recorded after 60, 408 and 125 600 min after the ion milling, with the peak of the latter spectrum returning to the position of that in the spectrum in the  $p$ -type material before the milling. This meant that in the long term the milling-induced defects did not affect optical properties of MCT.

Temperature- and excitation power-dependent modulated PL spectroscopy was used in Shanghai Institute of Technical Physics for the study of optical signatures of mercury vacancies and arsenic in MCT. First, Yue *et al.* [33] studied shallow levels in the MBE-grown material with  $x = 0.3$ . Samples grown on GaAs substrates (MCT/GaAs) were studied; of those, two samples, which Yue *et al.* [33] named as M1 ( $x = 0.300$ ) and M3 ( $x = 0.308$ ) were doped with arsenic with concentration  $\sim 10^{17} \text{ cm}^{-3}$ . Sample M1 and undoped sample M2 ( $x = 0.304$ ) were subjected to AA annealing, while sample M3 was subjected to VF annealing. As a result of the annealings, sample M3 had  $n$ -type conductivity due to a decrease in the concentration of  $V_{\text{Hg}}$ , while samples M1 and M2 had  $p$ -type conductivity due to the presence of shallow acceptors  $As_{\text{Te}}$  and  $V_{\text{Hg}}$ , respectively. The PL spectra of sample M1 exhibited a peak associated with interband transitions and another peak associated with  $c$ - $A$  transitions to the  $As_{\text{Te}}$  acceptor. The ionization energy of this acceptor was 11 meV, which corresponded to the previously obtained values. For sample M2, two peaks were observed that were separated by  $\sim 14$  meV; this was taken as the ionization energy of  $V_{\text{Hg}}$ . The PL spectra of the  $n$ -type sample M3 exhibited a number of lines associated with various impurity levels. The

fundamental peak, which was present in the spectra at any excitation energies and temperatures, was taken as the one due to interband transitions. Two other peaks were identified as  $D$ - $\nu$  (donor-to-VB with the donor being  $As_{\text{Hg}}$ ) transition and DAP ( $As_{\text{Hg}}-V_{\text{Hg}}$ ) recombination. The next peak was separated from the latter by 10.5 meV and appeared in the spectra only at low temperatures and low excitation energies. Its origin was ascribed to the optical transitions from the donor level to an acceptor-like complex ‘ $As_{\text{Hg}}-V_{\text{Hg}}$ ’. The energies of shallow levels detected in the samples, including  $As_{\text{Hg}}$  (donor),  $As_{\text{Te}}$ ,  $V_{\text{Hg}}$ , and the ‘ $As_{\text{Hg}}-V_{\text{Hg}}$ ’ complex (acceptors) were found to be 8.5, 11.0, 14.5 and 25.0 meV, respectively, and the forming energy of the complex was assessed as 10.5 meV. Identification of the defects responsible for the appearance of specific peaks was helped by the use of the data from the literature, which were obtained with electrical measurements and *ab initio* calculations [21,34,35].

Studies of impurity and defect levels in MCT doped with arsenic were continued by Yue *et al.* in Ref. [36]. PL spectra of five MBE-grown samples with  $x \approx 0.3$  were studied, with three of the samples (M1 to M3) being cut from the same wafer, sample M4 being vacancy-doped and the exact origin of sample M5 remaining unclear. The PL spectrum of the as-grown sample M1 ( $x = 0.298$ ) was the most rich for lines and purportedly showed seven different peaks  $A$  to  $G$  (Fig. 3a). These were indicative of the presence of some shallow and two deep energy states within the bandgap. The latter (corresponding to peaks  $F$  and  $G$  in Fig. 3a) represented levels with ionization energy of  $\sim 77$  meV and  $\sim 95$  meV, respectively. These were preliminarily ascribed to the transitions involving arsenic-related clusters or interstitials, i.e., arsenic atoms which did not occupy the proper position in the MCT lattice. This assumption was based on the fact that these levels were only typical for as-grown films and disappeared in the annealed samples, independent of arsenic activation; these levels have not been observed by Yue *et al.* in vacancy-

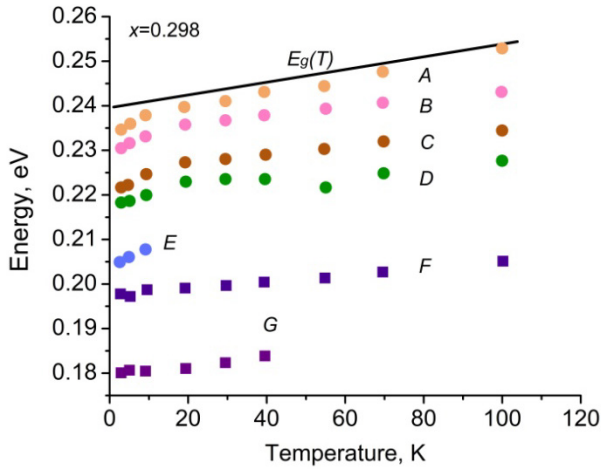


**Fig. 4.** Temperature dependence of PL peak energy for as-grown MCT sample with  $x = 0.298$  and calculated  $E_g(T)$  dependence (replotted using the data from Ref. [36]).

doped MBE-grown films either. The shallow levels were ascribed to defects such as  $V_{Hg}$ ,  $As_{Hg}$  and ' $As_{Hg}-V_{Hg}$ ', previously known from Ref. [33], and antisite tellurium  $Te_{Hg}$  (with  $D$ - $\nu$  type of optical transition). The ionization energy of  $Te_{Hg}$  was assessed as  $\sim 20$  meV. The spectrum of the annealed sample M2 contained only two peaks  $H$  and  $I$  separated by 11.0 meV (Fig. 3b); the second peak  $I$ , according to the annealing strategy (285 °C for 16 h plus 240 °C for 48 h) and secondary-ion mass-spectroscopy (SIMS) data was identified as the one originating in optical transitions involving  $As_{Te}$  acceptor.

The temperature dependences of the peak energies for the as-grown sample M1 (spectrum shown in Fig. 3a) are shown in Fig. 4. At higher temperatures ( $T > 10$  K), all the peaks with the exception of peak  $E$  depended on the temperature almost linearly. Non-linear dependence of the peak energy at  $T < 10$  K was interpreted as originating in the effect of band-tail states or localization of excitons.

Yet another vacancy-doped sample with  $x = 0.303$  was added to the study of arsenic doping-related issues in MCT by Yue *et al.* in Ref. [37]. The sample was annealed in vacuum at 360 °C for 16 h without addition of mercury vapors. At  $T = 11$  K the PL spectrum of the sample contained two lines, one being bandgap-related and the other one being clearly caused by  $c$ - $A$  transitions with the acceptor being  $V_{Hg}$ . The ionization energy for this acceptor was 14.5 meV. As discussed in the Introduction, the main goal of Ref. [37] and many other PL studies was to find the best path to activate arsenic in MBE-grown *in situ* doped MCT. The conclusion by Yue *et al.* in Ref. [37] was that the use of high activation temperature (such as 400 °C and higher) during AA annealing could produce a large number of excessive mercury vacancies and deteriorate the quality of epitaxial films. According to Yue *et al.*, after using such a high annealing temperature, recombination through  $V_{Hg}$  levels becomes dominant in PL as compared to recombination through arsenic-related levels. The low AA annealing temperature of 285 °C seemed to be more effective in activating the arsenic in terms of preserving the intrinsic advantages of the low growth temperature of MBE.

The PL studies by the Chinese authors discussed above were summarized in Refs. [38,39]. Fig. 5 represents schematics of electronic structure in MBE-grown *in situ* arsenic-doped MCT with  $x \approx 0.3$  for as-grown sample and samples after VF and AA+VF annealings redrawn after the original chart by Yue *et al.* [38]. In this chart, the positions of the deep levels  $D^{d1}$  and  $D^{d2}$  (Fig. 5a) were specified as 72 meV and 90 meV, respectively, below the conduction band, so they were identified as donors. It was noted that optical transitions involving these levels disappeared both after VF and AA+VF annealing, regardless of whether arsenic was activated or not. Also, it was stressed that the excessive mercury vacancies produced by higher

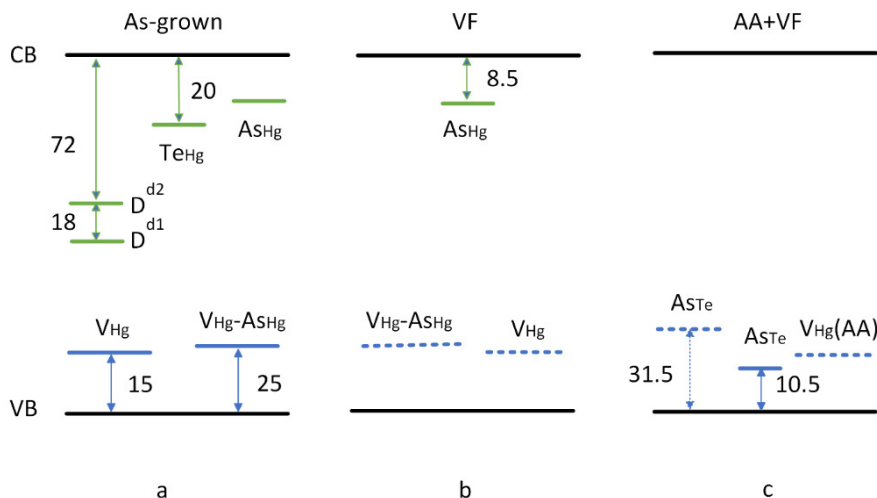


**Fig. 5.** Electronic structure of MCT with  $x = 0.3$  after Ref. [38]. Values are given in meV.

activation temperature were seemingly ‘increasing’ the chemical composition of the films (by moving bandgap-related peak towards higher energies), and this increase could not be eliminated completely by VF annealing. The energy levels of  $As_{Hg}$ ,  $Te_{Hg}$ , and  $V_{Hg}$  were specified to be 17 meV (previously 8.5 meV), 26 meV (previously 20 to 27 meV), and 12 meV (previously  $\sim 14.5$  meV), respectively [39]. These values were very close to the corresponding values obtained in the infrared PR studies by Shao *et al.* [40,41], while the difference in respect to the values obtained with PL earlier was explained by the fact that the analysis performed in Ref. [39] suggested that for neither as-grown nor annealed material it was not the interband transitions that took the dominant role in PL intensity at  $T < 100$  K (and even 200 K). The general conclusion related to defects in arsenic-doped MCT was that though conventional AA+VF annealing (400 °C for 0.5 h plus 240 °C for 48 h) was certainly capable of eliminating deep-level impurity-related PL features and changing the role of arsenic atoms from donors to acceptors, it did not eliminate  $V_{Hg}$  and  $Te_{Hg}$ .

Another question was related to the homogeneity of arsenic doping of MBE-grown films. This issue was addressed by Shao *et al.* in Ref. [42], where excitation from the back side (substrate side) of the samples was used in PL and PR experiments to study the vertical (along the growth direction) uniformity of composition and arsenic doping. The 8  $\mu\text{m}$ -thick epitaxial film had  $x = 0.23$ . AA annealing was performed at 300 °C for 16 h (which might indicate that the results of AA annealing presented in Refs. [38,39] were considered), and VF annealing, at 240 °C for 48 h. Both PL ( $T = 77$  K) and PR ( $T = 78\text{--}110$  K) measurements were performed with back-side and front-side excitation. A 1064 nm laser was used as an excitation source, and back-side excitation power was set twice as much as the front-side one to compensate the optical losses in the substrate. Front-side PL spectra were recorded at two different spots on the surface of the film with no difference found, which was indicative of good lateral uniformity of the sample. Both back-side and front-side PL spectra contained four lines. The HE lines were identified as  $c$ - $\nu$  transitions with energy difference of 1.3 meV between the front-side and back-side spectra, which was indicative of a change of 0.001 in the  $x$  value. The remaining lines of the front-side spectrum were identified as  $c$ -A1 ( $V_{Hg}$ ),  $c$ -A2 ( $As_{Te}$ ) and D1- $\nu$  ( $Te_{Hg}$ ) transitions. Those of the back-side spectrum were ascribed to  $c$ -A1 ( $V_{Hg}$ ) and to the mixture of transitions involving  $c$ -A2 ( $As_{Te}$ ) and D2- $\nu$  ( $As_{Hg}$ ) and that of D2-A1 ( $As_{Hg}$ -to- $V_{Hg}$ ) and D1- $\nu$  ( $Te_{Hg}$ ). The PR spectra appeared to be even more complicated, and their interpretation required following their evolution with temperature. In summary, the back-side PL and PR spectra indicated the co-existence of  $As_{Te}$  and  $As_{Hg}$ , while the front-side spectra showed full

activation of arsenic atoms as  $As_{Te}$  acceptors and high concentration of  $V_{Hg}$  as compared to the back side of the film. This suggested that AA annealing probably did not activate arsenic for the whole thickness of the film, while VF annealing was not capable of bringing  $V_{Hg}$  concentration at the front side to a low level found at the back side, i.e., close to the substrate. In regards to the alloy composition, the energy difference between the front-side and back-side PR spectra (4.6 meV) was slightly larger than that of PL (1.3 meV, as mentioned above). Shao *et al.* [42] seemed to incline to rely more on the PL data, which meant that they found a difference in  $x$  value of just 0.001.

A different kind of PL study was performed by Zhu *et al.* in Ref. [43]. The study was related to investigation of PL of MCT/CdTe heterostructures, which naturally form in MBE-grown material at the interface between the MCT film and the CdTe protecting/passivating cap layer and/or the film and the CdTe substrate (or buffer layer in the case of foreign substrate such as GaAs or Si). Zhu *et al.* [43] conducted PL measurements in ‘reflection’ mode on three  $4 \times 100$  nm = 400 nm-thick CdTe/ZnTe-passivated MCT films grown on GaAs substrates with CdTe buffer layers. In two samples with thicknesses  $\sim 3$   $\mu\text{m}$  and  $\sim 6$   $\mu\text{m}$ , respectively, besides the normal ‘edge’ bandgap PL, above-bandgap PL features were recorded at low temperatures ( $T < 100$  K). These features began to dominate as temperature was decreasing, in parallel to an abnormal reduction of the ‘edge’ PL line. The sample with very thick ( $\sim 10$   $\mu\text{m}$ ) MCT film and a 6  $\mu\text{m}$ -thick sample with the passivation layer removed demonstrated only bandgap-related PL lines. By analyzing the energies, temperature dependences, integral intensities and interference patterns, the above-bandgap PL features were ascribed to the MCT/CdTe interfacial transitions involving electrons in the former and holes in the latter. This interpretation seems very plausible, yet the authors of this review should like to note that it raises one important point. Namely, to explain the energy separation values between the bandgap-related PL peaks and above-bandgap ones, Zhu *et al.* [43] had to assume that the valence band offset (VBO) between MCT and CdTe was  $\sim 70$  and  $\sim 90$  meV for  $x = 0.314$  and  $x = 0.244$ , respectively. Indeed, there used to be some controversy in relation to VBO between HgTe and CdTe which, according to various sources, spanned from 40 to 800 meV [44–47]. We may note, however, that for a long time, according to Shih *et al.* [48], it was believed that the maximum of VB in HgTe lied higher than that in CdTe by 350 meV and this discontinuity was assumed to vary linearly with composition. The most recent, most often cited and used value of VBO between CdTe and HgTe at 0 K according to Becker *et al.* [49] is even bigger, 570 meV. Lower VBO values from Refs. [44–47] were obtained much earlier (before 1995) and cannot be fully

trusted, similar to the case of the values of the bandgap of MCT, as discussed in Ref. [3]. Considering the dependence of the VBO on the temperature and MCT composition established by Becker *et al.* [49], for the heterostructures studied by Zhu *et al.* at 5 K one could obtain values of the offset as 0.43 eV ( $x = 0.314$ ) and 0.39 eV ( $x = 0.244$ ). In the experiment, Zhu *et al.* [43] actually observed a distance between peaks of 0.140 and 0.065 eV for compositions  $x = 0.244$  and  $x = 0.314$ , respectively, which were at least three times smaller values. Zhu *et al.* [43] indeed noted that the mechanism of above-band-gap PL could be complicated and might be also related to factors such as fixed charges and polarization at the interface. Still, the results by Zhu *et al.* [43] raised some questions in relation to VBO between HgTe and CdTe.

The matter of the correct optical identification of the bandgap of MCT with  $x = 0.3$  in the presence of defect and impurity states was further raised in Refs. [12,50]. Wang *et al.* [12] compared the results of optical studies of LPE-grown vacancy-doped films and arsenic-doped and vacancy-doped MBE-grown films with the thickness of  $\sim 10 \mu\text{m}$ . From the optical transmission (OT) spectra recorded at different temperatures, an *S*-shaped temperature dependence of the transmission edge (as seen on ‘transmission vs energy’ plot) was obtained for the LPE-grown film, and it was noted that such dependence was previously typical of the MBE-grown samples and was associated with the effect of shallow acceptor states of  $V_{\text{Hg}}$ . The low-temperature PL spectrum of LPE-grown film exhibited two peaks: the first corresponded to interband transitions, and the second, shifted by  $\sim 11.5 \text{ meV}$ , to  $V_{\text{Hg}}$ -related transitions. The interband-related peak at 10 K was red-shifted as compared to calculated  $E_g$  (following Chu *et al.* [51]) by  $\sim 27 \text{ meV}$ , but this shift diminished as the temperature increased. On a ‘energy vs temperature’ plot, the *S*-shaped temperature dependence of the transmission edge turned into an *N*-shaped dependence (Fig. 6): up to  $T \sim 40 \text{ K}$  for the vacancy-doped LPE-grown film it had a different slope from that of  $E_g(T)$ , but for the arsenic-doped film, it followed  $E_g(T)$  rather closely. After 80 K both dependences began to basically follow  $E_g(T)$ , being separated from the latter by the energy of the order of 10 meV. The temperature shift for the PL spectra here equaled  $280 \mu\text{eV/K}$  for the LPE-grown sample and  $250 \mu\text{eV/K}$  for the MBE-grown film. For the transmission spectra, these values were  $171 \mu\text{eV/K}$  and  $196 \mu\text{eV/K}$ , respectively.

A theoretical analysis of the evolution of the Stokes shift for the transmission edge was performed, and a temperature dependence of the Fermi level  $E_F$  position in doped MCT with  $x = 0.3$  was calculated. The conclusion by Wang *et al.* [12] was that the shallow levels in doped MCT indeed induce the non-monotonous evolution of the absorption edge with temperature, and the degree of

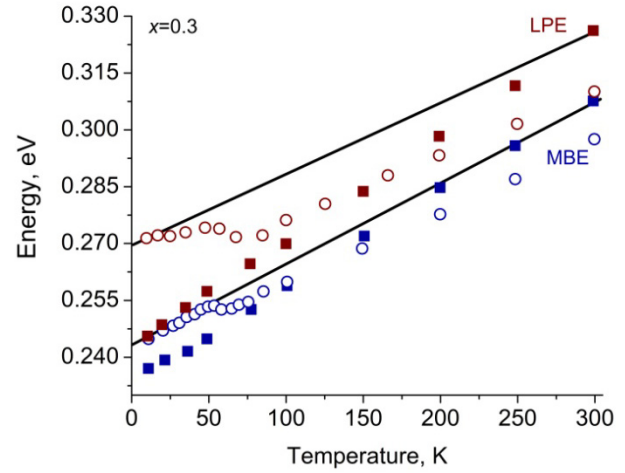


**Fig. 6.** Temperature dependences of optical bandgap according to optical absorption (open circles) and HE PL peaks (filled squares) data and  $E_g(T)$  according to Chu *et al.* [51] (lines) for MCT films with  $x \approx 0.3$  grown by LPE and MBE (replotted using the data from Ref. [12]).

the shift is mainly determined by the activation energy of the levels while the critical temperature for this effect (in the case of the samples considered, it equaled 150 K for the vacancy-doped sample and 120 K for the arsenic-doped one) was essentially influenced by the doping level. As a result, a conclusion was made that for the doped MCT, for assessing the bandgap, only the low-temperature ( $T < 10 \text{ K}$ ) absorption spectra can be employed, as the absorption edge at the typically used temperatures of 77 K or 300 K can be affected by the activation of shallow defects/impurities levels. In contrast to that, the PL assessment of the bandgap should be done at high temperature, i.e., 300 K, because at low temperatures the PL transitions relate to the excitonic effect and the tail of states produces the red-shift of the spectra in relation to the actual  $E_g$ . This conclusion and those made earlier in relation to optimal arsenic activation conditions (AA annealing at  $\sim 285 \text{ }^\circ\text{C}$  vs  $400 \text{ }^\circ\text{C}$ ) were confirmed by Shao *et al.* [50] with one more sample added to the study, a piece of a bulk MCT crystal with  $x = 0.225$ . On the basis of the results of the attempts to determine  $E_g$  with OT, PR, PC and PL, Shao *et al.* [50] stressed out that the transmission or absorption measurements can be used for the assessment of the bandgap value only in intrinsic MCT, while for the material with any kind of doping, all the methods yield a smaller  $E_g$  (and, correspondingly, chemical composition  $x$ ) due to the red-shift of the optical spectra caused by the effect of defect/impurity levels or band-tail states.

Finally, PL was involved in a study, where Qiu *et al.* [52] carried out a structural and optical analysis of MCT samples that differed in the temperature of MBE process. The films were grown on (211)GaAs substrates with ZnTe/CdTe buffers using solid CdTe sources instead of Cd

and Te sources. It was found that the film grown at 151 °C had better structural quality than a similar film grown at 155 °C. In addition to the poor quality of the former, many defects and micro-twins were found at its interface with the substrate. Interestingly, the authors observed only one peak in the PL spectra for both samples over the entire temperature range studied (9–290 K). These peaks were used to obtain the composition of the samples, which was also assessed using FTIR. The FTIR and PL measurements (at unspecified temperatures) gave very close values of  $x$ , which equaled 0.309 and 0.298 for the low- and high-temperature-grown samples, respectively. The FWHMs of the PL peaks were 19.2 meV and 25.2 meV for these samples, respectively, which once again indicated the difference in their structural quality. The slopes of the temperature dependences of the position of the PL peak differed from that of the calculated  $E_g$  (195  $\mu\text{eV/K}$ ) and equaled 269  $\mu\text{eV/K}$  and 275  $\mu\text{eV/K}$ , respectively, for the high- and low-temperature-grown samples, in consistency with the previous studies of the MBE-grown material.

Optical studies of MCT at the Institute of Microstructure Physics (IMP) in Russia were mostly aimed at obtaining stimulated emission: first, from the epitaxial films, and later, from the dedicated laser structures. The first cycle of works was performed in 2004–2014 [53–60] and was related to the study of the emission from the films and structures with potential wells with no effect of size quantization. These films were grown by MOCVD [53,54] or MBE on GaAs or Si (MBE only) [55–60] substrates with CdTe (MOCVD) or ZnTe/CdTe (MBE) buffer layers. A Nd:YAG laser emitting at 1064 nm [53–55] or wavelength-tunable OPO (optical parametric oscillator) emitting at 400–2500 nm [56–60], both operating in a pulse mode, were used as the PL excitation source. Variable-temperature PL measurements were performed in the temperature range 12–300 K. Spectra of spontaneous emission were mostly recorded just for determination of the value of the threshold power density for the stimulated emission, so those were not analyzed in much detail [53–56]. Still, it should be noted that it was Ref. [53] that marked the beginning of the ‘new era’ of PL studies in MCT mentioned above. Later papers by this group at IMP were devoted purely to stimulated emission [57–60].

The next cycle of optical studies of MCT at IMP started in 2012 with the investigations of spectra and kinetics of PC in narrow-gap ( $x < 0.2$ ) epitaxial films [61] and QW heterostructures [62] grown by MBE at Rzhannov Institute of Semiconductor Physics in Novosibirsk. The work soon turned into an extended study of stimulated emission from the QW heterostructures, and later, from bespoke MCT-based laser structures designed for both long- and middle IR ranges (for the latest results on the topic at the time of writing of this review, see, e.g., Refs. [63,64]). In the meantime,

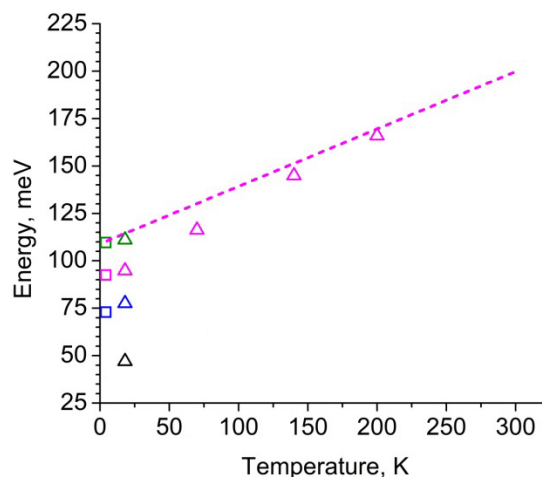


**Fig. 7.** Position of PL peaks (triangles) and 50% of PC intensity at the PC edge (squares) for films with  $x = 0.189, 0.210, 0.223$  and  $0.230$  taken from original spectra in Ref. [65]. Solid line is  $E_g(T)$  plotted for  $x = 0.223$  according to Ref. [51] and is shown as a guide for the eyes only.

a study of interband PL from epitaxial films at wavelengths up to 26  $\mu\text{m}$  was performed [65]. In that study, PL and PC were used to investigate MBE-grown heteroepitaxial films with  $0.19 < x < 0.23$ . The films were grown on (013)GaAs substrates using ZnTe/CdTe buffer layers, and the ‘active’ part of the structure was surrounded by 100–500 nm-thick graded gap MCT layers. PL studies were carried out in 18–200 K temperature range in a closed-cycle cryostat optically connected to a FTIR spectrometer. For PL excitation, a mechanically chopped (0.4–4.0 kHz) beam of a continuous wave Ti:Sapphire laser ( $\lambda = 800$  nm) was used. The samples were excited from the top of the film by normally incident laser beam and the PL signal was collected from the side of the substrate. To reduce the effect of the room temperature background radiation, a ‘double modulation’ technique similar to that proposed earlier by Shao *et al.* [24,25] was employed. PL and PC spectra were recorded at 18 K and 4.2 K, and the maxima of the PL peaks were in a good agreement with the edge of the PC spectra measured for the same samples. Figure 7 summarizes the data of these PL and PC measurements; the plot was built by the authors of this review on the basis of the spectra presented by Morozov *et al.* in Ref. [65]. As can be seen, as in the most cases of  $E_{\text{PL}}(T)$  dependences discussed above and in Ref. [3], the slope of  $E_{\text{PL}}(T)$  differs from that of  $E_g(T)$  (taken from Ref. [51] as an example and not used in Ref. [65]) at the low temperatures, but  $E_{\text{PL}}$  seem to approach the  $E_g$  as the temperature increases.

Morozov *et al.* [65] also noted a significant difference between the experimental and calculated values for PL line FWHM at 18 K (4–6 meV and 1.55 meV, respectively). With temperature increasing, however, the

experimental FWHM in  $k_B T$  units was decreasing, until at  $T \approx 70$  K it became equal to  $\sim 2$  for all samples and did not change significantly with further increase in the  $T$  value. According to Morozov *et al.* [65], this meant that at low temperatures the FWHMs of the PL lines were affected by the presence of the additional shallow impurity/defect, while at  $T > 70$  K, with FWHM in  $k_B T$  units approaching the theoretical limit, the spectrum was dominated by inter-band transitions of free carriers. The results of the study of the PC kinetics showed that the main recombination mechanism at high excitation levels in the studied samples was related to radiative transitions rather than Auger processes. This obviously opened the pathway to the studies of lasing in very long-wavelength MCT-based waveguide QW structures, such as presented in Ref. [63]. Still, the most outstanding result by Morozov *et al.* [65], in our opinion, was the detection, for the first time ever, of PL signal from a very narrow-gap MCT, with the PL peak wavelength located as far as  $26 \mu\text{m}$ .

Most recently, PL spectra in the THz domain were recorded by the same group [66–68]. For a nominally undoped MCT film with  $x = 0.19$ , two lines were found in the PL spectra, whose position did not change with temperature from 18 to 100 K, while PL intensity changed non-monotonically with temperature increasing. These lines were located in the range 5–12 meV and 16–25 meV, respectively and were attributed to the capture of free holes on the states of mercury vacancy, a double-charged acceptor [66]. PL lines with close energies were also found in MCT-based QW structures [66,67]. The PL spectrum of nominally undoped MCT film with  $x = 0.22$  recorded at  $T = 20$  K had two maxima corresponding to photon energies of  $\sim 7.2$  meV and  $\sim 10.4$  meV, respectively [68]. The spectral position of the latter was in a good agreement with the maximum of the PC spectrum of the  $p$ -type sample obtained from the same structure upon PT annealing, and this PL line dominated in the PL spectrum recorded at  $T = 5$  K. Kozlov *et al.* [68] believed that these two lines corresponded to intra-center transitions associated with mercury vacancy.

PL studies of MCT at Ioffe Institute, which started back in 1978 [3], came to a stop in 1991 and were resumed only in 2007 [69]. The subject of the investigation was now heteroepitaxial films grown on (013)GaAs or (013)Si substrates using the same MBE technology as in Refs. [55–68]. PL was studied in the temperature range  $4.2 \text{ K} < T < 300 \text{ K}$  under pulsed excitation with a  $1.03 \mu\text{m}$  semiconductor laser and detection with a cooled InSb photodiode (or Ge photodiode for short wavelengths). The upper side of heteroepitaxial structure was excited, and the PL was recorded from the substrate side. First, Ivanov-Omskii *et al.* [69] studied relatively wide-bandgap films ( $x \sim 0.6$ ), which emitted in the  $1.5\text{--}1.8 \mu\text{m}$

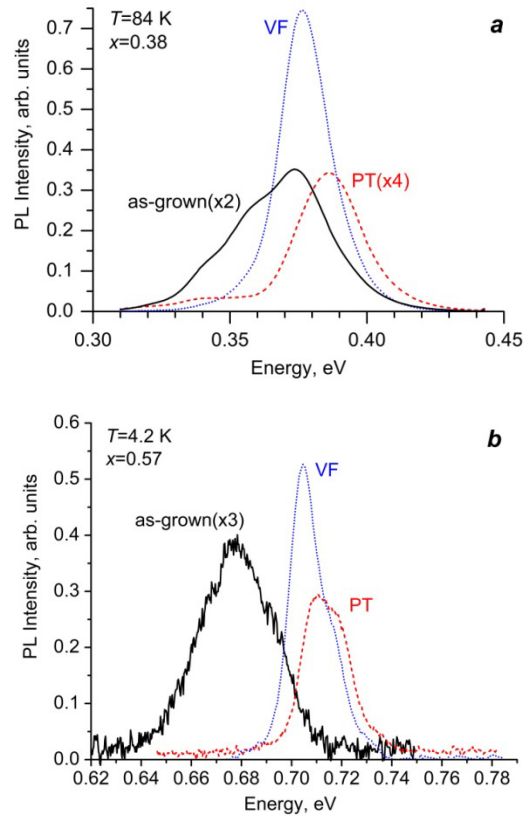


**Fig. 8.** PL spectra of two MCT films recorded on as-grown samples and samples subjected to PT and VF annealings (replotted using the data from [70,71]).

wavelength range. It was noted that PT annealing (20 h at  $270^\circ\text{C}$  in helium atmosphere) resulted in changes in the position of the PL spectrum, its FWHM, and the intensity of luminescence. These changes were attributed to increasing homogeneity of the heteroepitaxial film composition along its thickness as a result of the mutual diffusion of alloy components during the annealing. An increase in the room-temperature PL intensity for annealed films was ascribed to an improvement in the structure of the films.

The next studies were devoted to the investigation of the effect of various post-growth treatments (including PT and VF annealings and low-energy ion etching) on the optical properties of the material with  $x \sim 0.4$  [70] and  $x \sim 0.6$  [71]. In a study performed by a Russian-Ukrainian collaboration, Izhnin *et al.* [70] established that from those three types of the treatments, VF annealing was optimal for improving the PL characteristics (spectral composition, PL band intensity and FWHM) of the samples. Figure 8 represents PL spectra of MCT samples studied by Izhnin *et al.* [70] ( $T = 84 \text{ K}$ ) and Ivanov-Omskii *et al.* [71] ( $T = 4.2 \text{ K}$ ) and illustrates these findings. As can be seen, e.g., for the sample with  $x = 0.38$  [70], the maximum of the PL band in respect to the as-grown sample in the annealed samples was blue-shifted by 11 meV upon PT annealing and by 2 meV upon VF annealing (Fig. 8a). In both cases, the PL bands of annealed

samples exhibited narrowing that was more pronounced in the case of VF annealing, after which the spectra had the clear shape of a single line; the PL intensity also increased significantly following this treatment. After PT annealing, the PL spectrum of the material with  $x = 0.38$  acquired a significant long-wavelength component in addition to the main peak. Similar changes in the shape and position of emission band in the PL spectrum as a result of annealing were observed for all other MCT samples with  $x \sim 0.4$  studied in Ref. [70], and a very close pattern for PL spectra evolution upon annealing was observed for sample with  $x = 0.57$  by Ivanov-Omskii *et al.* in Ref. [71] at  $T = 4.2$  K (Fig. 8b).

A blue-shift of the PL peak immediately after ion etching with subsequent red-shift upon relaxation discussed above [26,27,32] (see also Ref. [72] by Pociask *et al.*), was observed and explained by the BM effect associated with formation of donor complexes involving interstitial mercury atoms  $Hg_i$  released during the etching, and disintegration of the complexes with time.

In the studies such as presented in Refs. [70,71], it was noted that the PL peak almost in the whole temperature range explored ( $4.2 < T < 300$  K) lied lower in energy than the calculated bandgap (calculated according to Laurenti *et al.* [73]) by a certain value  $\delta E$  that depended on temperature. It was natural to attribute this effect to the composition fluctuations, i.e., alloy disorder. Ivanov-Omskii *et al.* [71] indeed attributed the PL peaks to recombination of excitons localized at composition non-homogeneities, and carried out an analysis that provided a way for the evaluation of the non-homogeneity measure. This analysis was based on the model of light absorption and emission in semiconductors with band gap fluctuations initially developed by Mattheis *et al.* for Cu(In,Ga)Se<sub>2</sub> films [74], and was also used for interpreting PL spectra in MCT by Gemain *et al.* in Ref. [18]. The amplitude of the non-homogeneities was shown to decrease by about 50% as a result of both PT and VF annealings [71]. The value of the PL line FWHM after the annealings was close to that calculated under an assumption of purely stochastic fluctuations in MCT sample with  $x = 0.38$ , but remained twice as much for the sample with  $x = 0.57$ . In a conference paper by Ivanov-Omskii *et al.* [75] it was also noted that for the latter case, the energy of the PL peak  $E_{PL}$  increased with the temperature increasing, while the bandgap energy should have been decreasing. Later, the authors of Refs. [73,75] and related articles developed their own model of the effect of composition fluctuations on radiative recombination in MCT [76]. The model was based on wave packet principles and dealt with the relaxation and recombination of photo-excited carriers in a medium with large-scale potential fluctuations. The model adequately described the effect of

composition fluctuations on the recombination in a sense that it yielded reasonable broadening and the red-shift of the PL spectra with the increase in the scale of fluctuations, but was not employed to describe experimental data quantitatively.

Ivanov-Omskii *et al.* also reported on the results of PL and PC measurements performed on MCT-based structures with 50 to 200 nm-wide potential wells [77]. These structures emitted at wavelengths 2.8–3.8  $\mu\text{m}$  at 300 K. Their PL spectra at low temperatures were found to be strongly affected by the effect of alloy disorder, too, which led to a substantial red-shift of the emission spectrum in relation to the calculated bandgap of the material in the wells. As in the case of epitaxial films, this effect could also be reduced by post-growth annealing of the structures, which also increased the luminescence intensity. The bandgap values determined as the energy of the HE PL peak at 300 K and the energy at 50% of the PC signal agreed with each other and with the ellipsometric data obtained *in situ* during the growth. Size quantization effect in these structures was not observed.

The results of the study of PL of films grown on silicon substrates (MCT/Si) showed that the compositional disorder in them did not exceed that in the films grown by the same method on GaAs substrates [78]. In contrast to the latter, the PL spectra of the former exhibited emission lines due to DAP recombination and the recombination of excitons bound to impurities. The results obtained at Ioffe Institute in 2007–2010 on MBE-grown MCT/GaAs films and potential-well structures and MCT/Si films were summarized in a sort of self-review in Ref. [79]. It was confirmed that for heteroepitaxial films with  $x = 0.33$ – $0.40$ , low-temperature VF annealing reduced the alloy disorder down to stochastic composition fluctuations. For structures with  $x > 0.5$ , the disorder remained significant upon annealing. These results are illustrated in Fig. 9, which shows temperature dependences of the peak position of the high energy PL band for some of the studied samples. The same figure presents  $E_g(T)$  dependences for MCT with the corresponding composition (for the as-grown structures) calculated according to Laurenti *et al.* [73].

It can be seen that at low temperatures ( $T < 100$  K), the studied samples exhibited a slope of the temperature run of  $E_{PL}$  that was different from that of the  $E_g(T)$ . In addition, a non-monotonic run of  $E_{PL}$  was observed at  $4.2 < T < 20$  K for the structures under study: namely the  $E_{PL}(T)$  dependence had a minimum at  $T \approx 12$ – $15$  K. These features were naturally attributed to the fact that the PL spectra were dominated by the line of the radiative recombination of excitons localized in the density-of-states tails. A comparative analysis of properties of the films grown on GaAs and Si substrates as well as of the structures with potential wells grown in various epitaxy modes allowed

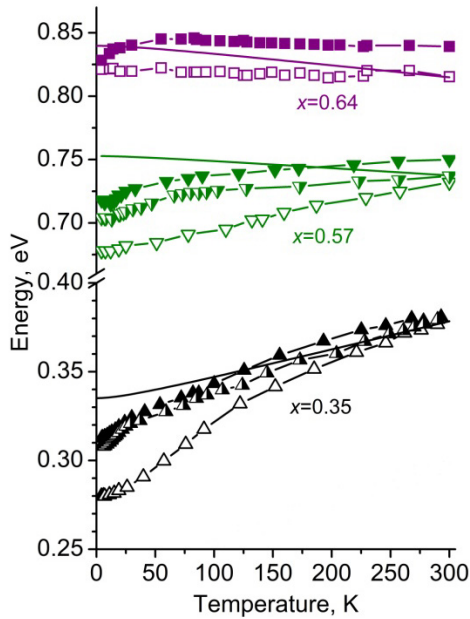


**Fig. 9.** Temperature dependences of the energy position of the HE PL peaks for three MCT films. Empty symbols correspond to as-grown films; filled symbols, to films subjected to PT annealing; half-filled symbols, to films subjected to VF annealing. Solid curves show calculated  $E_g(T)$  dependence for the corresponding MCT composition (replotted using the data from Ref. [79]).

for suggesting that the observed disorder was mostly due to the non-equilibrium nature of MBE. The effect of a substrate and, in particular, by that made of silicon, was manifested in the appearance of recombination channels related to acceptor centers. Size quantization effects for potential-well structures was observed only for those with  $x = 0.33$  in the well.

PL studies were also employed for assessing, again by the Russian-Ukrainian collaboration involving Izhnin *et al.*, the quality of MCT films with  $x \approx 0.20$ – $0.29$  grown by LPE on (111)CdZnTe substrates [80]. The main investigation tool used in that study was electrical measurements (those of the Hall coefficient and conductivity) in combination with ion etching. This etching releases  $Hg_I$  atoms that actively interact with existing defects and change the properties of the material [28,29,31,32]. By measuring the parameters of the material before and after the etching, as well as during the relaxation, when etching-induced defects gradually disintegrate, it is possible to obtain a considerably larger body of information about the defect structure of the material, compared with the ‘standard’ electrical measurements [29]. For example, Izhnin *et al.* showed that it was possible to use this technique to determine the concentration of residual donors, an important parameter of the material that could not be measured using the conventional Hall-effect measurements due to electrical compensation [81]. Moreover, by creating a  $Hg_I$  concentration exceeding the equilibrium value by six to seven

orders of magnitude, the etching can somehow activate even neutral defects in MCT [29]. In the case of Ref. [80] by Izhnin *et al.*, PL was studied at  $T = 84$  K in films with  $x = 0.27$  and  $x = 0.29$ . The PL signal was excited by a semiconductor laser with a wavelength of  $0.81 \mu\text{m}$  and excitation power of  $120 \text{ W/cm}^2$ ; the laser beam was mechanically chopped at a frequency of 192 Hz. The relatively high power of excitation (‘strong excitation mode’) in these experiments made it possible to assume that the HE peaks of the PL bands were associated with interband recombination, and to compare the peak energies to calculated bandgap values. The experimentally observed  $E_{PL}$  was in good agreement with  $E_g$  values for MCT with corresponding compositions. The PL spectrum of the film with  $x = 0.27$  contained ME and LE bands spaced by  $\sim 13$  and  $\sim 18$  meV, respectively, from the HE band, and presumably associated with acceptor states. These bands were observed both before and after the etching, which was indicative of the fact that the acceptor states which they were associated with formed no donor complexes with  $Hg_I$  (and thus were not related to mercury vacancies). The position of all peaks after the etching and relaxation remained the same.

A similar combination of electrical and optical methods was applied to MBE-grown MCT/Si films in the study presented by Izhnin *et al.* in Ref. [82]. The electrical studies showed that the concentration of residual donors in these films ( $(3\text{--}8) \times 10^{14} \text{ cm}^{-3}$ ) was much lower than that in the MCT/GaAs films. As-grown MCT/Si films, however, contained considerable density of stacking faults, which affected the carrier mobility. The stacking faults were eliminated in a sort of PT annealing at  $230 \text{ }^\circ\text{C}$ ; that annealing also helped to reduce the compensation typical of the as-grown films. The successive ion etching yielded the films with electrical parameters close to those of the MCT bulk crystals of the best possible quality. Still, the PL spectra of the as-grown samples, annealed samples and samples after ion etching appeared to be almost identical in terms of the position of the spectra (with one band only) and their FWHMs. The latter at  $T = 84$  K equaled 15–17 meV.

In contrast to the films studied by Izhnin *et al.* in Ref. [82], low-temperature PL spectra of most of the MCT/Si films studied by the same collaboration in Ref. [83] revealed bands related to acceptor states. Time-resolved PL measurements made it possible to identify, in some as-grown samples, PL bands associated with DAP recombination. The spectra of other samples contained bands that could be related to  $c\text{--}A$  transitions for acceptors with activation energy of 20 to 40 meV. Izhnin *et al.* [83] believed that those bands were not related to a mercury vacancy on the basis of the fact that for the latter the characteristic ionization energy was  $\sim 15$  meV, and such band

was clearly observed in the spectra of samples subjected to PT annealing.

Acceptor states immune to annealing and/or ion etching were also found by Izhnin *et al.* in some MCT/GaAs films [84]. On that occasion, the LE PL lines of as-grown samples corresponded to acceptors with activation energy of 14 to 18 meV. Ion milling alone did not change the PL spectrum of these films, yet PT annealing increased the distance between the HE and LE bands from 18 to 26 meV with the subsequent ion etching removing the LE band completely. Izhnin *et al.* [84] suggested that the acceptor defect in question was related to a structural imperfection which would be typical specifically of MCT/GaAs. We may note that suitable candidates for such structural defects have been recently identified in MBE-grown MCT/GaAs as misoriented micro-regions, which strongly affected carrier lifetime via introduction of Shockley–Read–Hall recombination centers [85]; it is quite possible that that type of defects introduces not only deep levels, but also shallow ones.

In the studies discussed above an interesting phenomenon was noted down, which was a relatively strong PL signal from narrow-bandgap MCT at the room temperature. This phenomenon was not observed in the earlier PL studies of this material [3]: typically, the PL signal gradually disappeared above 120–200 K, depending on the chemical composition of the studied material. This PL quenching was attributed to fundamental process of Auger recombination, and, as such, could not be hoped to be overcome by simply ‘improving the quality’ of the material. However, modern heteroepitaxial structures grown by MBE easily exhibited emission at 300 K [15,39,79,86,87], which seemingly represented a sort of a puzzle. So, an issue of high-temperature PL from MBE-grown MCT was specifically addressed in application to epitaxial films with  $x = 0.29–0.64$  [88] and to 50–1000 nm-thick potential wells with composition of the material in the well  $x = 0.23–0.45$  [89], respectively. These studies included samples investigated earlier with the addition of some new structures. For most of the structures, the low-temperature ( $4.2 < T < 100$  K) PL spectra contained a single Gaussian-shaped line, but closer to room temperatures, a considerable broadening and distortion of the shape of the spectra was found; some spectra at 300 K seemed to contain additional lines with peak energy exceeding the material bandgap. One of the most remarkable effects observed during those studies was unexpectedly small decrease in the PL intensity with temperature increasing from 77 to 300 K. This effect was ascribed to localization of carriers at potential fluctuations induced by the technology-related alloy disorder specific to MBE as a non-equilibrium growth method. Once again, it was noted that annealing of the samples typically led to significant increase in the PL

intensity and decrease in the spectral line FWHM. On a technical note, it should be mentioned that PL registration methods in the IR range greatly improved since the early days of MCT technology, and part of the success in detecting high-temperature PL from MCT can be attributed to this progress.

In Ref. [90], Izhnin *et al.* revisited the subject of PL properties of MCT subjected to ion etching. It was noted that the etching itself seemingly never had any effect on the position of the HE PL band in MCT in contrast to annealing (be it PT or VF type), which always led to a noticeable blue shift of the HE peak. From this observation, it followed that the introduction of a large number of Hg<sub>I</sub> atoms into MCT could not by itself change the energy of interband transitions. It was concluded then, that the pronounced transformation of MBE-grown MCT as a result of annealings, as manifested in the shift of the PL peak and narrowing of the exciton emission band as discussed above, was due to the diffusion of components and ordering of the solid solution rather than to defect–impurity reactions in the system of point defects in the mercury sublattice. The evolution of the PL spectra of the samples subjected first to the annealing and then to ion etching, in its turn, suggested that in the as-grown samples acceptor impurities were present in the form of defect/impurity complexes. Thermal annealing caused their dissociation with a change in the depth of the acceptor levels as detected in the PL studies, and then, during the course of the etching, these defects/impurities would react with Hg<sub>I</sub> atoms and lose their acceptor properties. This strongly suggested that combination of PL studies with annealing/ion etching could be employed for diagnostics of the defect structure of the MCT similar to the already shown effectiveness of combination of measurements of electrical properties with various types of post-growth treatments.

The next cycle of works at the Ioffe Institute was primarily devoted to the study of acceptors in MBE-grown MCT [91–95]. One of the reasons for this study was the development of the  $p^+–n$ -type photodiodes, which are characterized by much lower dark currents than their  $n^+–p$  counterparts. This eventually provides for a higher working temperature of the diodes and is explained by a longer lifetime of minority carriers in  $n$ -type MCT, since this material has a lower concentration of deep recombination centers controlling the lifetime [96]. Refs. [91,92] dealt with MCT/Si films with  $0.35 < x < 0.39$  and thickness of 5–7  $\mu\text{m}$ . Some samples were doped with indium (to  $\sim 10^{15}$   $\text{cm}^{-3}$ ) while the other remained intentionally un-doped. The general challenge associated with those samples was that the measurements of their electrical characteristics upon post-growth processing revealed some anomalies. In particular, while the samples annealed in PT annealing mode showed quite expectable

results, which was conversion to  $p$ -type with hole concentration at 77 K  $p_{77} = (1.5\text{--}3)\times 10^{16} \text{ cm}^{-3}$  and mobility  $\mu_p = 150\text{--}250 \text{ cm}^2/(\text{V}\cdot\text{s})$ , arsenic implantation and AA annealing of some films led to conversion to  $p$ -type over the entire thickness of the sample rather than to the formation of a thin  $p^+$ -region, and thus, of a  $p^+n$  junction. PL studies performed on the as-grown material, samples subjected to PT annealing, implantation and AA annealing, as well as cycling annealing aimed at annihilation of dislocations, showed that the material under study was characterized by the presence of uncontrolled acceptors. Experiments with chemical etching of some of the material showed that the acceptors responsible for the appearance of deep ( $\sim 55 \text{ meV}$ ) levels were located at the surface of the structures, whereas shallow ( $\sim 11 \text{ meV}$ ) acceptors were distributed over the entire volume of the films. In Ref. [94], the range of compositions of MCT/Si structures studied with PL was extended to  $0.30 < x < 0.40$ , and the energy ranges of shallow and deep acceptor levels observed were determined as  $20\text{--}30 \text{ meV}$  and  $50\text{--}60 \text{ meV}$ , respectively. At the same time, the analysis of the temperature dependence of the minority carrier lifetime demonstrated that it was controlled by levels with  $\sim 30 \text{ meV}$  energy. This could very well mean that these levels were associated with mercury vacancies, as the  $\sim 30 \text{ meV}$  deep donor-like levels are characteristic of vacancy-doped  $p$ -type MCT and indeed control the value of carrier lifetime in the material [97]. Yet in Ref. [94],  $\sim 30 \text{ meV}$  levels were detected in both the  $p$ - and  $n$ -type samples, and in the last case the energy level of recombination centers upon low-excitation-intensity measurements of lifetime should be calculated from the top of the valence band. It was noted that these levels disappeared from the spectra of samples subjected to AA annealing, which includes a high-temperature stage that is known to reduce the concentration of structural defects in MBE-grown MCT [82]. This allowed the authors of Ref. [94] to conclude that the acceptor levels they found could be associated with impurities and/or intrinsic defects localized at structural defects. Interestingly, for deeper levels in MCT/Si, optical transitions could be very weakly expressed at low ( $T = 4.2 \text{ K}$ ) and high ( $T > 150 \text{ K}$ ) temperatures, but became clearly pronounced at temperatures near  $60 \text{ K}$ , as is illustrated in Fig. 10.

In Ref. [93], the results of similar studies were reported for MCT/GaAs films with  $0.30 < x < 0.39$ . These investigations showed that while such films grown under ‘optimal’ conditions typically exhibited only bandgap-related PL band, in films that experienced conditions of a mercury deficiency upon epitaxy and/or post-growth processing, specific acceptor states with energy depths of  $\sim 18$  and  $\sim 27 \text{ meV}$  were found. The former were associated with a complex of defects that could be destroyed by heat treatment, and the latter seemingly formed as a result of the

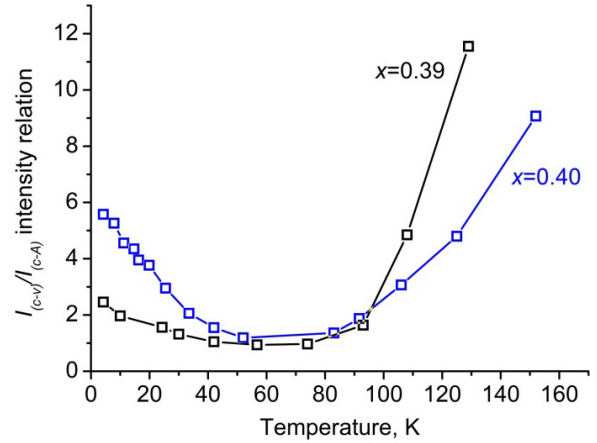


**Fig. 10.** Temperature dependence of the relation of intensity of PL interband recombination line  $I_{(c-v)}$  to that of a transition to a deep acceptor level  $I_{(c-A)}$  for two as-grown MCT/Si films with  $x \sim 0.4$  (replotted using the data from Ref. [95]).

destruction of the complex. The authors of Ref. [93] attributed the crucial role in the formation of the complexes to the mercury vacancy. It was concluded that formation of the acceptor states was determined by some features of the MBE modes used for the growth of the films and was not related to the specifics arising from the use of a silicon substrate.

The results of the PL studies of MCT/Si and MCT/GaAs films grown by MBE were summarized in Ref. [98]. Once again, a difference between the defect structures of these two types of films as revealed with PL was underlined. Indeed, MCT/GaAs films grown under the optimal growth conditions were mostly free of defect-related energy levels within the bandgap, which was confirmed by lifetime measurements. A mercury deficiency during the growth or post-growth treatment resulted in the formation of vacancy-related defects with energy levels  $14, 18$  and/or  $27 \text{ meV}$ , depending on the defect type. The properties of MCT/Si films appeared to be always affected by uncontrolled point defects, producing both shallow ( $\sim 12 \text{ meV}$  and from  $20$  to  $35 \text{ meV}$ ) and deep (from  $\sim 50$  to  $\sim 70 \text{ meV}$ ) energy levels. At least part of these defects could not be associated with mercury vacancies, so point defects localized at structural defects were suggested as possible candidates. The post-growth annealing was found to be able not only to reduce the allow disorder in the as-grown MCT, but also to decrease the concentration of acceptor levels in MCT/Si.

The next three cycles of studies of PL in MBE-grown MCT at Ioffe Institute were related to the material with a specific chemical composition. First, material with  $x \sim 0.5$  was studied by Timoshkov *et al.* [99]. MCT with  $x \approx 0.5$  is a sort of ‘exotic’ material, but at the moment it attracts considerable interest due to the development of photodetectors for the so-called ‘extended Short-Wave IR’,

eSWIR range ( $\lambda = 1.7\text{--}3.0\ \mu\text{m}$ ) for astronomy applications [100,101]. Both MCT/Si and MCT/GaAs films with  $x$  varying from 0.47 to 0.57 were investigated by Timoshkov *et al.* in Ref. [99]. The experimental PL spectra were related to those obtained with calculations performed according to Bazhenov *et al.* [102], and it was shown that the studied films indeed possessed substantial fluctuations of chemical composition. These data were compared to those taken from the literature (and discussed in detail in Ref. [3]) and it was concluded that the observed effect was typical of MCT with  $x \sim 0.5$  in general, and was not specific of a given growth technology.

The next cycle of studies was devoted to the material with  $x \sim 0.3$ . Here, films with a thickness from 5 to 9  $\mu\text{m}$  and  $x \sim 0.35$  were studied first, with some of them demonstrating ‘abnormal’ behavior, which consisted in very strong shift of OT edge upon annealing [103,104]. Low-temperature PL studies showed that at  $T = 4.2\ \text{K}$  for such as-grown sample the FWHM of the HE line was almost twice as large ( $\sim 34\ \text{meV}$ ) as that typical of ‘normal’ MCT/GaAs films ( $< 20\ \text{meV}$ ). Also, the ‘abnormal’ sample demonstrated a huge ( $\sim 60\ \text{meV}$ ,  $\sim 20\%$  of  $E_g$  value) blue-shift of the PL spectrum after PT annealing. Still, the FWHM after this annealing decreased down to 14 meV, typical of ‘normal’ films. According to the PL spectra recorded on the sample with the etched surface layer, this ‘abnormality’ was not related to compositional non-uniformities along the growth direction. In the course of X-ray diffraction (XRD) studies it was found that diffraction signals both before and after the annealing for the ‘abnormal’ sample, in contrast to ‘normal’ samples, were very weak [104]. This obviously was indicative of low crystalline quality that could not be improved by the annealing. Ivanov-Omskii *et al.* in Ref. [103] made an attempt to attribute the observed abnormalities to the effect of infamous ‘V-defects’, which are known to be surrounded by a polycrystalline phase that can transform during annealing [105]. Later, however, Andryushchenko *et al.* [104] found that the density of these defects in the ‘abnormal’ sample did not exceed that typical of MBE-grown MCT. In relation to the usefulness of PL studies in MCT, which is the subject of this review, it was concluded that optical properties of MBE-grown MCT films were not strictly related to the structural quality of the material.

Next, MCT samples with  $x \sim 0.7$  grown by various methods were subjected to comparative optical and structural studies [106–108]. MBE-grown material of this kind is now demanded for use in barrier, spacer and waveguide layers in multi-QW (MQW)-based MCT lasers (see, e.g., [63,64]). At the same time, MCT with  $x > 0.6$  has never been studied in detail, as photodetectors operating at the corresponding wavelengths (0.8–1.5  $\mu\text{m}$ ) can be easily made from less expensive and more

technologically advanced III–V semiconductors. MBE-grown samples involved in the studies in Refs. [106–108] included heteroepitaxial films, MQW (with a well width  $< 10\ \text{nm}$ ) and single potential-well (with well widths from 50 to 200 nm) structures containing material with  $x = 0.68\text{--}0.78$ . For comparison, films grown by LPE and a sample of bulk crystal grown by vertically-directed crystallization with the replenishment from the solid phase were studied. A considerable degree of alloy disorder was found in MBE-grown material, which was expressed in different slopes and even signs of  $dE_{\text{PL}}/dT$  for the samples with very similar chemical composition. FWHMs of the HE PL lines at  $T = 4.2\ \text{K}$  for the studied material with  $x \approx 0.7\text{--}0.8$  (16–25 meV) somewhat exceeded those for MBE-grown MCT with  $x \approx 0.3\text{--}0.4$  (10–15 meV), but were comparable, or even smaller than the FWHMs of the HE PL lines for samples with  $x \approx 0.5\text{--}0.6$  (15–30 meV) as studied by Timoshkov *et al.* in Ref. [99]. At that, no direct relation between the structural properties of the material with  $x \approx 0.7$ , as assessed with XRD, and the scale of the disorder was found. PL studies revealed defect states in the bandgap with energies  $\sim 10\text{--}12\ \text{meV}$ ,  $\sim 25\text{--}30\ \text{meV}$  and  $\sim 70\ \text{meV}$ . As those were not typical of MBE-grown MCT/GaAs films with smaller values of  $x$ , it was concluded that their formation was related to growth conditions rather than to the defects formed due to a specific lattice mismatch, as was the case for MCT/Si. Perhaps, it was something to be expected, as optimal temperatures of MBE of CdTe and narrow-bandgap MCT (not to mention HgTe) differ [105], and growing a sequence of CdTe and HgTe layers represents a real challenge [109,110]. The resulting compromise in growth conditions may easily negatively affect the quality of the material both in the QWs and in the wider-bandgap layers, and how this translates into the properties of MCT-based MQW structures is something yet to be studied.

A similar study was performed by Andryushchenko *et al.* for MCT/GaAs and MCT/Si samples with  $x \sim 0.3$  [111,112]. Optical and structural properties of films grown by MBE, LPE, MOCVD, and of a sample of bulk crystal were studied and compared. The composition of the material varied from 0.29 to 0.32. Interestingly, for the MCT/Si films no bands associated with acceptor energy states were found. The shape and the FWHM for MBE-, LPE- and bulk-grown samples at 85 K were similar (from 13 to 20 meV). FWHMs of MOCVD-grown films were much larger ( $\sim 30\ \text{meV}$ ), and the  $E_{\text{PL}}$  of the latter at  $T > 100\ \text{K}$  exceeded the calculated bandgap of the material with the corresponding composition. This, and the large FWHMs of the PL peaks for these films were attributed to the specifics of growth technology, the so-called ‘Interdiffusion Multilayer Process’, where very thin CdTe and HgTe layers are

deposited consequently and interdiffuse as the growth proceeds [113]. For other types of material at low temperatures  $E_{\text{PL}}$  was smaller than the calculated  $E_{\text{g}}$ , which was indicative of the effect of compositional fluctuations. As in the case with MBE-grown films with  $x \sim 0.7$ , for the films with  $x \sim 0.3$  no direct relation between the structural properties, as studied with XRD, and the scale of the alloy disorder as revealed by the PL studies, was found.

Concluding this part of the review, we may start with an observation that inconsistencies in the properties of the material investigated in different studies, which seemed to be very strong at the early stages of the development of MCT, at the later stages seemed to reduce. Though French and Chinese groups performed their studies using the material grown ‘in house’, Russian groups and the Russian-Ukrainian collaboration headed by Izhnin studied MBE-grown material obtained from the same source, Rzhano Institute of Semiconductor Physics in Novosibirsk. This made comparison of the results of different groups a bit easier than it was in Ref. [3]. Some uncertainties still remain, but we can briefly summarize this part of the review as follows:

- 1) It is clear that applying the results of PL studies for the assessment of the bandgap in MCT is a dangerous idea. At low temperatures, the energy of emitted photons will always be smaller than the actual (‘nominal’) bandgap due to the effect of compositional fluctuations. Some research groups put more emphasis on that than the others, but the actual data presented in the literature speak for themselves. At that, the uncertainty in determining the exact energy gap of MCT remains, different research groups continue to use different  $E_{\text{g}}(x,T)$  formulae, so the direct comparison between the results remains challenging. At temperatures close to the room temperatures on most occasions the position of the PL spectra seemed to reflect the actual bandgap; however, in some cases the spectra contained lines that lied higher in energy than  $E_{\text{g}}$  [43,88,89,112].
- 2) The good news, however, is that now there is no necessity to use PL studies for the determination of  $E_{\text{g}}$  in MCT (as in many other materials). For a number of years luminescence has remained an important tool for fulfilling this task, yet modern technology offers a wide range of other methods for the precise determination of the bandgap as such. As MCT remains a material of choice for IR photodetectors [114], absorption-related optical methods appear to be much more important in this realm than PL. With the advent of MCT-based interband lasers [63,64], PL studies gain back some importance as a material study tool, but these devices seem to be far from practical implementation.
- 3) The relation between the structural quality of MCT as determined with ‘structural’ methods such as XRD and PL is not quite clear. For a close-to-ideal crystal, the parameters determined with PL studies, such as FWHM of the fundamental PL line, should be indeed characterizing the structural quality of the material. With MCT being a solid solution with strong compositional fluctuations and a lot of intrinsic defects, this relation is not so obvious. Therefore, a standard phrase of the like “PL represents a good tool for assessing the structural quality of material”, which was used in many early MCT papers, cannot be recommended for use anymore. More research is certainly needed in this respect.
- 4) As mentioned in the introduction to this part of the review, PL studies now play important role in the studies of defects in MCT, especially those related to *p*-type doping. Basically, the problem of *in situ p*-type doping of MCT remains unresolved, which explains why modern photodetectors are still based on outdated ion implantation technology, and the lack of direct-injection MCT-based IR emitters. Two most likely candidates for shallow acceptor in MCT are still the mercury vacancy and the arsenic dopant, and PL studies performed in the last ~15 years revealed the following:
  - a) Mercury vacancy. There remains a discrepancy on the optical signature(s) of  $V_{\text{Hg}}$  in MCT. While some works state that mercury vacancy yields a single shallow level in the bandgap (12 to 18 meV according to different sources [13,33,37,39,50,52]), latest results from the French and the IMP Russian groups are indicative of the fact that  $V_{\text{Hg}}$  can produce at least two optically detectable energy states, ~11 and ~27 meV for  $x = 0.33$  and ~17 and 36 meV for  $x = 0.45$ , according to Ref. [16,17], or ~10 and ~20 meV, barely dependent on material composition, for  $x \sim 0.2\text{--}0.3$ , according to, e.g., Ref. [11]. This may be in a sense confirmed by the research performed by the Ioffe Institute group, where the conditions of mercury deficiency lead to the appearance of two acceptor levels, ~18 meV and ~27 meV, which were seemingly not representing pure  $V_{\text{Hg}}$  (which was attributed a ~14 meV level) but were somehow associated with it [93]. At that, the understanding of site configuration of double-level  $V_{\text{Hg}}$  in MCT lattice differs: while the French group consider the vacancy to be a ‘negative-U’ center, which is supposedly confirmed by EXAFS measurements and some calculations, the IMP group base their conclusion on the existence of a ‘classical’ double acceptor  $V_{\text{Hg}}$  on the results of the PC studies and thoroughly developed theoretical model. One other

seeming controversy in relation to  $V_{\text{Hg}}$  is the results of PL studies of MCT subjected to ion etching. This treatment should eliminate vacancies almost completely. Yet PL spectra of ion-etched MCT seem to contain suspiciously large number of defect-related lines, and some of them could be ascribed to  $V_{\text{Hg}}$ -related transitions. This issue needs to be addressed in a more systematic way.

- b) Arsenic acceptor. There is still some controversy related to arsenic acceptor optical signatures in MBE-grown MCT. The only consensus that seems to exist relates to the fact that arsenic doping does not lead to the formation of just two defects such as  $\text{As}_{\text{Hg}}$  and  $\text{As}_{\text{Te}}$ . Most certainly, many other defects and complexes form as by-products of arsenic doping and activation annealing in MCT, and these may include such exotic structures as acceptor  $\text{AsHg}_8$  and donor  $\text{As}_2\text{Te}_3$  [18]. Co-existence of large number of defects (which may also include antisite tellurium  $\text{Te}_{\text{Hg}}$ , also formed in the course of activation) gives much freedom for interpreting optical transitions in arsenic-doped MCT. Still, there is no doubt that optical (and PL, in particular) studies of arsenic-doped MCT greatly helped in searching the optimal doping strategy (such as, e.g., lowering the activation annealing temperature [38,39]), and gave an advanced insight into dopant incorporation in this material.
- 5) Deep levels (~70 and ~90 meV) found in arsenic-doped MCT samples were also attributed to by-products of arsenic activation in Ref. [38] and were identified as donors. However, deep levels with ~70 meV energy were found on numerous occasions in undoped MBE-grown MCT [98,108], and earlier, in the material grown by other methods [3]. As these levels were typical of both wide-bandgap MCT/GaAs films, which were grown under ‘non-optimal’ conditions and MCT/Si films, one can suppose that they may be somehow related to structural imperfections rather than to doping. Regarding donor levels in MCT as such, there is still some controversy in relation to whether they can actually be deep enough to be detected with optical measurements.
- 6) Acceptor levels. Wide variety of acceptor levels in the ranges 10–15 meV and 20–35 meV was found in the studies reviewed above, and while most of them can indeed be attributed to vacancy or arsenic-related (in the case of doped samples) defects, there may be a possibility that some of them are associated with other defects. This matter should be a subject of further investigations.

Concluding, we can observe that the potential that PL studies offer in relation to the studies of general properties of MCT as well in solving particular tasks (such as vacancy or arsenic doping or optimization of MBE parameters) is far from being exhausted. We can express the hope that many interesting studies are lying ahead, and that they will duly serve the advancement of MCT technology.

## ACKNOWLEDGEMENTS

The support from the Ministry of Science and Higher Education of the Russian Federation (agreement nr. 075-15-2021-1349) is kindly acknowledged.

## REFERENCES

- [1] V.I. Ivanov-Omskii, B.T. Kolomiets, A.A. Mal'kova, *Optical and Photoelectric Properties of HgTe and Its Alloys with CdTe*, Sov. Physics – Solid State, 1964, vol. 6, no. 5, pp. 1140–1143.
- [2] J. Chu, Y. Chang, *Optical Properties of MCT*, Chapter 9, in: *Mercury Cadmium Telluride: Growth, Properties and Applications*, ed. by P. Capper, J.W. Garland; Wiley, New York, 2010, pp. 205–238.
- [3] M.S. Ruzhevich, K.D. Mynbaev, *Photoluminescence in Mercury Cadmium Telluride — A Historical Retrospective. Part I: 1966-1996*, Rev. Adv. Mater. Technol., 2020, vol. 2, no. 4, pp. 47–64.
- [4] M.A. Kinch, *The future of infrared; III-Vs or HgCdTe?* J. Electron. Mater., 2015, vol. 44, no. 9, pp. 2969–2976.
- [5] J.W. Garland, C. Grein, S. Sivananthan, *Arsenic p-doping of HgCdTe grown by molecular beam epitaxy (MBE): A solved problem?* J. Electron. Mater., 2013, vol. 42, no. 11, pp. 3331–3336.
- [6] K.D. Mynbaev, V.I. Ivanov-Omskii, *Doping of Epitaxial Layers and Heterostructures Based on HgCdTe*, Semiconductors, 2006, vol. 40, no. 1, pp. 1–21.
- [7] B. Delacourt, P. Ballet, F. Boulard, A. Ferron, L. Bonnefond, T. Pellerin, A. Kerlain, V. Destefanis, J. Rothman, *Temperature and Injection Dependence of Photoluminescence Decay in Midwave Infrared HgCdTe*, J. Electron. Mater., 2017, vol. 46, no. 12, pp. 6817–6828.
- [8] L. Rubaldo, A. Brunner, J. Berthoz, N. Péré-Laperne, A. Kerlain, P. Abraham, D. Bauza, G. Reimbold, O. Grandidier, *Defects study in  $\text{Hg}_{1-x}\text{Cd}_x\text{Te}$  infrared photodetectors by deep level transient spectroscopy*, J. Electron. Mater., 2014, vol. 43, no. 8, pp. 3065–3069.
- [9] C.H. Swartz, R.P. Tomkins, N.C. Giles, T.H. Myers, D.D. Edwall, J. Ellsworth, E. Piquette, J. Arias, M. Berding, S. Krishnamurthy, I. Vurgaftman, J.R. Meyer, *Fundamental material studies of undoped, In-doped, and As-doped  $\text{Hg}_{1-x}\text{Cd}_x\text{Te}$* , J. Electron. Mater., 2004, vol. 33, no. 6, pp. 728–736.
- [10] F. Gemain, I.C. Robin, S. Brochen, M. De Vita, O. Grandidier, A. Lusson, *Optical and Electrical Studies of the Double Acceptor Levels of the Mercury Vacancies in HgCdTe*, J. Electron. Mater., 2012, vol. 41, no. 10, pp. 2867–2873.
- [11] V.V. Rummyantsev, D.V. Kozlov, S.V. Morozov, M.A. Fadeev, A.M. Kadykov, F. Teppe, V.S. Varavin, M.V. Yakushev, N.N. Mikhailov, S.A. Dvoretiskii, V.I. Gavrilenko, *Terahertz photoconductivity of double acceptors*

- in narrow gap HgCdTe epitaxial films grown by molecular beam epitaxy on GaAs(013) and Si(013) substrates, *Semicond. Sci. Technol.*, 2017, vol. 32, no. 9, art. no. 095007.
- [12] H. Wang, J. Hong, F. Yue, C. Jing, J. Chu, *Optical homogeneity analysis of Hg<sub>1-x</sub>Cd<sub>x</sub>Te epitaxial layers: How to circumvent the influence of impurity absorption bands?* *Infr. Phys. Technol.*, 2017, vol. 82, pp. 1–7.
- [13] I.C. Robin, M. Taupin, R. Derone, A. Solignac, P. Ballet, A. Lusson, *Photoluminescence studies of arsenic-doped Hg<sub>1-x</sub>Cd<sub>x</sub>Te epilayers*, *Appl. Phys. Lett.*, 2009, vol. 95, no. 20, art. no. 202104.
- [14] I.C. Robin, M. Taupin, R. Derone, A. Solignac, P. Ballet, A. Lusson, *Photoluminescence studies of HgCdTe epilayers*, *Phys. Status Solidi C*, 2010, vol. 7, no. 6, pp. 1615–1617.
- [15] I.C. Robin, M. Taupin, R. Derone, P. Ballet, A. Lusson, *Photoluminescence Studies of HgCdTe Epilayers*, *J. Electron. Mater.*, 2010, vol. 39, no. 7, pp. 868–872.
- [16] F. Gemain, I.C. Robin, M. De Vita, S. Brochen, A. Lusson, *Identification of the double acceptor levels of the mercury vacancies in HgCdTe*, *Appl. Phys. Lett.*, 2011, vol. 98, no. 13, art. no. 131901.
- [17] F. Gemain, I.C. Robin, G. Feuillet, *Composition dependence of the mercury vacancies energy levels in HgCdTe: Evolution of the “negative-U” property*, *J. Appl. Phys.*, 2013, vol. 114, no. 21, art. no. 213706.
- [18] F. Gemain, I.C. Robin, S. Brochen, P. Ballet, O. Gravrand, G. Feuillet, *Arsenic complexes optical signatures in As-doped HgCdTe*, *Appl. Phys. Lett.*, 2013, vol. 102, no. 14, art. no. 124104.
- [19] P. Ballet, B. Polge, X. Biquard, I. Alliot, *Extended X-ray Absorption Fine Structure Investigation of Arsenic in HgCdTe: the Effect of the Activation Anneal*, *J. Electron. Mater.*, 2009, vol. 38, no. 9, pp. 1726–1732.
- [20] X. Biquard, I. Alliot, P. Ballet, *Extended x-ray absorption fine structure study of arsenic in HgCdTe: p-type doping linked to nonsubstitutional As incorporation in an unknown AsHg<sub>8</sub> structure*, *J. Appl. Phys.*, 2009, vol. 106, no. 10, art. no. 103501.
- [21] M.A. Berding, A. Sher, *Amphoteric behavior of arsenic in HgCdTe*, *Appl. Phys. Lett.*, 1999, vol. 74, no. 5, pp. 685–687.
- [22] H.R. Vydyanath, *Amphoteric behaviour of group V dopants in (Hg, Cd)Te*, *Semicond. Sci. Technol.*, 1990, vol. 5, no. 3S, pp. S213–S216.
- [23] S.P. Guo, Y. Chang, J.M. Zhang, X.C. Shen, J.H. Chu, S.X. Yuan, *Effect of the post-As<sup>+</sup>-implantation thermal treatment on MBE HgCdTe optical properties*, *J. Electron. Mater.*, 1996, vol. 25, no. 4, pp. 761–764.
- [24] J. Shao, F. Yue, X. Lu, W. Lu, W. Huang, Z. Li, S. Guo, J. Chu, *Photomodulated infrared spectroscopy by a step-scan Fourier transform infrared spectrometer*, *Appl. Phys. Lett.*, 2006, vol. 89, no. 18, art. no. 182121.
- [25] J. Shao, W. Lu, X. Lu, F. Yue, Z. Li, S. Guo, J. Chu, *Modulated photoluminescence spectroscopy with a step-scan Fourier transform infrared spectrometer*, *Rev. Sci. Instrum.*, 2006, vol. 77, no. 6, art. no. 063104.
- [26] F.X. Zha, J. Shao, J. Jiang, W.Y. Yang, *“Blueshift” in photoluminescence and photovoltaic spectroscopy of the ion-milling formed n-on-p HgCdTe photodiodes*, *Appl. Phys. Lett.*, 2007, vol. 90, no. 20, art. no. 201112.
- [27] F.X. Zha, J. Shao, *The blue-shift effect of the ion-milling-formed HgCdTe photodiodes*, *Proc. SPIE*, 2008, vol. 6984, art. no. 69840G.
- [28] K.D. Mynbaev, V.I. Ivanov-Omskii, *Modification of Hg<sub>1-x</sub>Cd<sub>x</sub>Te properties by Low-Energy Ions (Review)*, *Semiconductors*, 2003, vol. 37, no. 10, pp. 1127–1150.
- [29] I.I. Izhnin, K.D. Mynbaev, A.V. Voitsekhovskii, A.G. Korotaev, O.I. Fitsych, M. Pociask-Bialy, *Ion etching of HgCdTe: properties, patterns and use as a method for defect studies*, *Opto-Electron. Rev.*, 2017, vol. 25, no. 2, pp. 148–170.
- [30] F. Yue, J. Shao, X. Lü, W. Huang, J. Chu, J. Wu, X. Lin, L. He, *Anomalous temperature dependence of absorption edge in narrow-gap HgCdTe semiconductors*, *Appl. Phys. Lett.*, 2006, vol. 89, no. 2, art. no. 021912.
- [31] I.I. Izhnin, K.D. Mynbaev, M. Pociask, R.Ya. Mudryy, A.V. Voitsekhovskii, N.Kh. Talipov, *Long-term room-temperature relaxation of the defects induced in (Hg,Cd)Te by low-energy ions*, *Physica B*, 2009, vol. 404, no. 23–24, pp. 5025–5027.
- [32] M. Pociask, I.I. Izhnin, K.D. Mynbaev, A.I. Izhnin, S.A. Dvoretzky, N.N. Mikhailov, Yu.G. Sidorov, V.S. Varavin, *Blue-shift in photoluminescence of ion-milled HgCdTe films and relaxation of defects induced by the milling*, *Thin Solid Films*, 2010, vol. 518, no. 14, pp. 3879–3881.
- [33] F. Yue, J. Chu, J. Wu, Z. Hu, Y. Li, P. Yang, *Modulated photoluminescence of shallow levels in arsenic-doped Hg<sub>1-x</sub>Cd<sub>x</sub>Te (x ≈ 0.3) grown by molecular beam epitaxy*, *Appl. Phys. Lett.*, 2008, vol. 92, no. 12, art. no. 121916.
- [34] L.Z. Sun, X. Chen, J. Zhao, J.B. Wang, Y.C. Zhou, W. Lu, *Electronic properties and chemical trends of the arsenic in situ impurities in Hg<sub>1-x</sub>Cd<sub>x</sub>Te: First-principles study*, *Phys. Rev. B*, 2007, vol. 76, no. 4, art. no. 045219.
- [35] Y.S. Ryu, Y.B. Heo, B.S. Song, S.J. Yoon, Y.J. Kim, T.W. Kang, T.W. Kim, *Optical and electrical properties of in situ-annealed p-type Hg<sub>0.7</sub>Cd<sub>0.3</sub>Te epilayers grown on CdTe buffer layers for applications as infrared detectors*, *Appl. Phys. Lett.*, 2003, vol. 83, no. 18, pp. 3776–3778.
- [36] F. Yue, J. Wu, J. Chu, *Deep/shallow levels in arsenic-doped HgCdTe determined by modulated photoluminescence spectra*, *Appl. Phys. Lett.*, 2008, vol. 93, no. 13, art. no. 131909.
- [37] F.-Y. Yue, L. Chen, J. Wu, Z.-G. Hu, Y.-W. Li, P.-X. Yang, J.-H. Chu, *Impurity Activation in MBE-Grown As-Doped HgCdTe by Modulated Photoluminescence Spectra*, *Chin. Phys. Lett.*, 2009, vol. 26, no. 4, art. no. 047804.
- [38] F.-Y. Yue, L. Chen, Y.-W. Li, Z.-G. Hu, L. Sun, P.-X. Yang, J.-H. Chu, *Influence of annealing conditions on impurity species in arsenic-doped HgCdTe grown by molecular beam epitaxy*, *Chinese Phys. B*, 2010, vol. 19, no. 11, art. no. 117106.
- [39] X. Zhang, J. Shao, L. Chen, X. Lu, S. Guo, L. He, J. Chu, *Infrared photoluminescence of arsenic-doped HgCdTe in a wide temperature range of up to 290 K*, *J. Appl. Phys.*, 2011, vol. 110, no. 4, art. no. 043503.
- [40] J. Shao, X. Lü, S. Guo, W. Lu, L. Chen, Y. Wei, J. Yang, L. He, J. Chu, *Impurity levels and bandedge electronic structure in as-grown arsenic-doped HgCdTe by infrared photoreflectance spectroscopy*, *Phys. Rev. B*, 2009, vol. 80, no. 15, art. no. 155125.
- [41] J. Shao, L. Chen, X. Lü, W. Lu, L. He, S. Guo, J. Chu, *Realization of photoreflectance spectroscopy in very-long wave infrared of up to 20 μm*, *Appl. Phys. Lett.*, 2009, vol. 95, no. 4, art. no. 041908.

- [42] J. Shao, L. Chen, W. Lu, X. Lü, L. Zhu, S. Guo, L. He, J. Chu, *Backside illuminated infrared photoluminescence and photorefectance: Probe of vertical nonuniformity of HgCdTe on GaAs*, Appl. Phys. Lett., 2010, vol. 96, no. 12, art. no. 121915.
- [43] L. Zhu, L. Chen, L. Zhu, Z. Qi, X. Chen, S. Guo, L. He, J. Shao, *Above-Hg<sub>1-x</sub>Cd<sub>x</sub>Te-bandgap photoluminescence and interfacial channels in Hg<sub>1-x</sub>Cd<sub>x</sub>Te–CdTe heterostructure*, Phys. Status Solidi B, 2016, vol. 253, no. 2, pp. 377–383.
- [44] Y. Guldner, G. Bastard, J. P. Vieren, M. Voos, J. P. Faurie, A. Million, *Magneto-Optical Investigations of a novel Superlattice: HgTe–CdTe*, Phys. Rev. Lett., 1983, vol. 51, no. 10, pp. 907–910.
- [45] Y.C. Chang, J.N. Schulman, G. Bastard, Y. Guldner, M. Voos, *Effects of quasi-interface states in HgTe–CdTe superlattices*, Phys. Rev. B, 1985, vol. 31, no. 4, pp. 2557–2560.
- [46] C.R. Becker, Y.S. Wu, A. Waag, M.M. Kraus, G. Landwehr, *The orientation independence of the CdTe–HgTe valence band offset as determined by X-ray photoelectron spectroscopy*, Semicond. Sci. Technol., 1991, vol. 6, no. 12C, pp. C76–C79.
- [47] Z. Yang, Z. Yu, Y. Lansari, S. Hwang, J.W. Cook, J.F. Schetzina, *Optical properties of HgTe/CdTe superlattices in the normal, semimetallic, and inverted-band regimes*, Phys. Rev. B, 1994, vol. 49, no. 12, pp. 8096–8108.
- [48] C.K. Shih, W.E. Spicer, *Determination of a natural valence-band offset: The case of HgTe–CdTe*, Phys. Rev. Lett., 1987, vol. 58, no. 24, pp. 2594–2597.
- [49] C.R. Becker, V. Latussek, A. Pfeuffer-Jeschke, G. Landwehr, L.W. Molenkamp, *Band structure and its temperature dependence for type-III HgTe/Hg<sub>1-x</sub>Cd<sub>x</sub>Te superlattices and their semimetal constituent*, Phys. Rev. B, 2000, vol. 62, no. 15, pp. 10353–10363.
- [50] F.-Y. Yue, S.-Y. Ma, J. Hong, P.-X. Yang, C.-B. Jing, Y. Chen, J.-H. Chu, *Optical characterization of defects in narrow-gap HgCdTe for infrared detector applications*, Chinese Phys. B, 2019, vol. 28, no. 1, art. no. 017104.
- [51] J.H. Chu, S.C. Xu, D.Y. Tang, *Energy gap versus alloy composition and temperature in Hg<sub>1-x</sub>Cd<sub>x</sub>Te*, Appl. Phys. Lett., 1983, vol. 43, no. 11, pp. 1064–1066.
- [52] X.-F. Qiu, S.-X. Zhang, J. Zhang, Y.-C. Zhu, C. Dou, S.-C. Han, Y. Wu, P.-P. Chen, *Microstructure and Optical Characterization of Mid-Wave HgCdTe Grown by MBE under Different Conditions*, Crystals, 2021, vol. 11, no. 3, art. no. 296.
- [53] Yu.N. Nozdrin, A.V. Okomel'kov, A.P. Kotkov, A.N. Moiseev, N.D. Grishnova, *Stimulated and Spontaneous Emission of Cd<sub>x</sub>Hg<sub>1-x</sub>Te Structures in the Range 3.2–3.7 μm at 77 K*, Semiconductors, 2004, vol. 38, no. 12, pp. 1374–1377.
- [54] Yu.N. Nozdrin, A.V. Okomel'kov, A.P. Kotkov, A.N. Moiseev, N.D. Grishnova, *Induced Emission from Cd<sub>x</sub>Hg<sub>1-x</sub>Te at a Wavelength of 3400 nm at 77 K*, JETP Letters, 2004, vol. 80, no. 1, pp. 23–25.
- [55] A.A. Andronov, Yu.N. Nozdrin, A.V. Okomel'kov, V.S. Varavin, R.N. Smirnov, D.G. Ikusov, *Spontaneous and Stimulated Emission from Cd<sub>x</sub>Hg<sub>1-x</sub>Te Semiconductor Films*, Semiconductors, 2006, vol. 40, no. 11, pp. 1266–1274.
- [56] A.A. Andronov, Yu.N. Nozdrin, A.V. Okomel'kov, N.N. Mikhailov, G.Yu. Sidorov, V.S. Varavin, *Stimulated emission from optically excited Cd<sub>x</sub>Hg<sub>1-x</sub>Te structures at room temperature*, J. Lumin., 2012, vol. 132, p. 612–616.
- [57] A.A. Andronov, Yu.N. Nozdrin, A.V. Okomel'kov, A.A. Babenko, V.S. Varavin, D.G. Ikusov, R.N. Smirnov, *Stimulated Radiation of Optically Pumped Cd<sub>x</sub>Hg<sub>1-x</sub>Te-Based Heterostructures at Room Temperature*, Semiconductors, 2008, vol. 42, no. 2, pp. 179–182.
- [58] A.A. Andronov, Yu.N. Nozdrin, A.V. Okomel'kova, V.S. Varavin, N.N. Mikhailov, G.Yu. Sidorov, *Stimulated Radiation at a Wavelength of 2.5 μm at Room Temperature from Optically Excited Cd<sub>x</sub>Hg<sub>1-x</sub>Te Based Structures*, Semiconductors, 2010, vol. 44, no. 4, pp. 457–462.
- [59] Yu.N. Nozdrin, A.V. Okomel'kov, V.S. Varavin, M.V. Yakushev, S.A. Dvoret'skii, *Dual Wavelength Stimulated Emission from a Double Layer Cd<sub>x</sub>Hg<sub>1-x</sub>Te Structure at Wavelengths of 2 and 3 μm*, JETP Letters, 2013, vol. 97, no. 6, pp. 358–361.
- [60] Yu.N. Nozdrin, A.V. Okomel'kov, V.S. Varavin, M.V. Yakushev, S.A. Dvoret'skii, *Simultaneous stimulated emission at two frequencies from Cd<sub>x</sub>Hg<sub>1-x</sub>Te semiconducting structure*, J. Lumin., 2014, vol. 151, pp. 197–200.
- [61] V.V. Rummyantsev, S.V. Morozov, A.V. Antonov, M.S. Zholudev, K.E. Kudryavtsev, V.I. Gavrilenko, S.A. Dvoret'skii, N.N. Mikhailov, *Spectra and kinetics of THz photoconductivity in narrow-gap Hg<sub>1-x</sub>Cd<sub>x</sub>Te (x < 0.2) epitaxial films*, Semicond. Sci. Technol., 2013, vol. 28, no. 12, art. no. 125007.
- [62] S.V. Morozov, M.S. Joludev, A.V. Antonov, V.V. Rummyantsev, V.I. Gavrilenko, V.Ya. Aleshkin, A.A. Dubinov, N.N. Mikhailov, S.A. Dvoret'skiy, O. Drachenko, S. Winner, H. Schneider, M. Helm, *Study of lifetimes and photoconductivity relaxation in heterostructures with Hg<sub>1-x</sub>Cd<sub>x</sub>Te/Cd<sub>y</sub>Hg<sub>1-y</sub>Te quantum wells*, Semiconductors, 2012, vol. 46, no. 11, pp. 1362–1366.
- [63] V.V. Rummyantsev, A.A. Dubinov, V.V. Utochkin, M.A. Fadeev, V.Ya. Aleshkin, A.A. Razova, N.N. Mikhailov, S.A. Dvoret'skiy, V.I. Gavrilenko, S.V. Morozov, *Stimulated emission in 24–31 μm range and «Reststrahlen» waveguide in HgCdTe structures grown on GaAs*, Appl. Phys. Lett., 2022, vol. 121, no. 18, art. no. 182103.
- [64] M.A. Fadeev, A.A. Dubinov, A.A. Razova, A.A. Yantser, V.V. Utochkin, V.V. Rummyantsev, V.Ya. Aleshkin, V.I. Gavrilenko, N.N. Mikhailov, S.A. Dvoret'skiy, S.V. Morozov, *Balancing the Number of Quantum Wells in HgCdTe/CdHgTe Heterostructures for Mid-Infrared Lasing*, Nanomaterials, 2022, vol. 12, no. 24, art. no. 4398.
- [65] S.V. Morozov, V.V. Rummyantsev, A.V. Antonov, K.V. Maremyanin, K.E. Kudryavtsev, L.V. Krasilnikova, N.N. Mikhailov, S.A. Dvoret'skii, V.I. Gavrilenko, *Efficient long wavelength interband photoluminescence from HgCdTe epitaxial films at wavelengths up to 26 μm*, Appl. Phys. Lett., 2014, vol. 104, no. 7, art. no. 072102.
- [66] D.V. Kozlov, V.V. Rummyantsev, S.V. Morozov, A.M. Kadykov, M.A. Fadeev, M.S. Zholudev, V.S. Varavin, N.N. Mikhailov, S.A. Dvoret'skii, V.I. Gavrilenko, F. Teppe, *Terahertz Photoluminescence of Double Acceptors in Bulky Epitaxial HgCdTe Layers and HgTe/CdHgTe Structures with Quantum Wells*, JETP, 2018, vol. 127, no. 6, pp. 1125–1129.
- [67] D.V. Kozlov, V.V. Rummyantsev, A.M. Kadykov, M.A. Fadeev, N.S. Kulikov, V.V. Utochkin, N.N. Mikhailov, S.A. Dvoret'skii, V.I. Gavrilenko, H.-W. Hubers, F. Teppe, S.V. Morozov, *Features of Photoluminescence of Double Acceptors in HgTe/CdHgTe Heterostructures with*

- Quantum Wells in a Terahertz Range*, JETP Letters, 2019, vol. 109, no. 10, pp. 657–662.
- [68] D.V. Kozlov, V.V. Rumyantsev, A.V. Ikonnikov, V.V. Utochkin, A.A. Razova, K.A. Mazhukina, N.N. Mikhailov, S.A. Dvoretzky, S.V. Morozov, V.I. Gavrilenko, *Non-Radiative Transitions of Holes on Mercury Vacancies in Narrow-Gap HgCdTe*, Photonics, 2022, vol. 9, no. 12, art. no. 887.
- [69] V.I. Ivanov-Omski, N.L. Bazhenov, K.D. Mynbaev, V.A. Smirnov, V.S. Varavin, A.A. Babenko, I.G. Ikusov, G.Yu. Sidorov, *1.5–1.8 μm photoluminescence of MBE-grown HgCdTe films*, Tech. Phys. Lett., 2007, vol. 33, no. 6, pp. 471–473.
- [70] A.I. Izhnin, I.I. Izhnin, K.D. Mynbaev, V.I. Ivanov-Omski, N.L. Bazhenov, V.A. Smirnov, V.S. Varavin, N.N. Mikhailov, Yu.G. Sidorov, *Effect of Annealing on the Optical and Photoelectrical Properties of Cd<sub>x</sub>Hg<sub>1-x</sub>Te Heteroepitaxial Structures for the Middle Infrared Range*, Tech. Phys. Lett., 2009, vol. 35, no. 2, pp. 147–150.
- [71] V.I. Ivanov-Omskii, N.L. Bazhenov, K.D. Mynbaev, *Effect of alloy disorder on photoluminescence in HgCdTe*, Phys. Status Solidi B, 2009, vol. 246, no. 8, pp. 1858–1861.
- [72] M. Pociask, I.I. Izhnin, A.I. Izhnin, S.A. Dvoretzky, N.N. Mikhailov, Yu. G. Sidorov, V.S. Varavin, K.D. Mynbaev, *Donor doping of HgCdTe for LWIR and MWIR structures fabricated with ion milling*, Semicond. Sci. Technol., 2009, vol. 24, no. 2, art. no. 025031.
- [73] J.P. Laurenti, J. Camassel, A. Bouhemadou, B. Toulouse, R. Legros, A. Lusson, *Temperature dependence of the fundamental absorption edge of mercury cadmium telluride*, J. Appl. Phys., 1990, vol. 67, no. 10, pp. 6454–6460.
- [74] J. Mattheis, U. Rau, J.H. Werner, *Light absorption and emission in semiconductors with band gap fluctuations — A study on Cu(In,Ga)Se<sub>2</sub> thin films*, J. Appl. Phys., 2007, vol. 101, no. 11, art. no. 113519.
- [75] V.I. Ivanov-Omskii, N.L. Bazhenov, K.D. Mynbaev, V.A. Smirnov, V.S. Varavin, N.N. Mikhailov, G.Yu. Sidorov, *Study of alloy disorder in (Hg,Cd)Te with the use of infrared photoluminescence*, Physica B, 2009, vol. 404, no. 23–24, pp. 5035–5037.
- [76] A.V. Shilyaev, K.D. Mynbaev, N.L. Bazhenov, A.A. Greshnov, *Effect of Composition Fluctuations on Radiative Recombination in Narrow-Gap Semiconductor Solid Solutions*, Tech. Phys., 2017, vol. 62, no. 3, pp. 441–448.
- [77] V.I. Ivanov-Omskii, K.D. Mynbaev, N.L. Bazhenov, V.A. Smirnov, N.N. Mikhailov, G.Yu. Sidorov, V.G. Remesnik, V.S. Varavin, S.A. Dvoretzky, *Optical properties of molecular beam epitaxy-grown HgCdTe structures with potential wells*, Phys. Status Solidi C, 2010, vol. 7, no. 6, pp. 1621–1623.
- [78] K.D. Mynbaev, N.L. Bazhenov, V.I. Ivanov-Omski, V.A. Smirnov, M.V. Yakushev, A.V. Sorochkin, V.S. Varavin, N.N. Mikhailov, G.Yu. Sidorov, S.A. Dvoretzky, Yu.G. Sidorov, *Photoluminescence of CdHgTe Epilayers Grown on Silicon Substrates*, Tech. Phys. Lett., 2010, vol. 36, no. 12, pp. 1085–1088.
- [79] K.D. Mynbaev, N.L. Bazhenov, V.I. Ivanov-Omski, N.N. Mikhailov, M.V. Yakushev, A.V. Sorochkin, S.A. Dvoretzky, V.S. Varavin, Yu.G. Sidorov, *Photoluminescence of Cd<sub>x</sub>Hg<sub>1-x</sub>Te Based Heterostructures Grown by Molecular-Beam Epitaxy*, Semiconductors, 2011, vol. 45, no. 7, pp. 872–879.
- [80] I.I. Izhnin, A.I. Izhnin, E.I. Fitsych, N.A. Smirnova, I.A. Denisov, M. Pociask, K.D. Mynbaev, *Defect Structure of Cd<sub>x</sub>Hg<sub>1-x</sub>Te Films Grown by Liquid-Phase Epitaxy, Studied by Means of Low-Energy Ion Treatment*, Semiconductors, 2011, vol. 45, no. 9, pp. 1124–1128.
- [81] I.I. Izhnin, K.D. Mynbaev, A.V. Voitsekhovskiy, A.G. Korotaev, O.I. Fitsych, M. Pociask-Bialy, S.A. Dvoretzky, *Background Donor Concentration in HgCdTe*, Opto-Electron. Review, 2015, vol. 23, no. 3, pp. 200–207.
- [82] I.I. Izhnin, A.I. Izhnin, H.V. Savytskyy, M.M. Vakiv, Y.M. Stakhira, O.E. Fitsych, M.V. Yakushev, A.V. Sorochkin, I.V. Sabinina, S.A. Dvoretzky, Yu.G. Sidorov, V.S. Varavin, M. Pociask-Bialy, K.D. Mynbaev, *Defect structure of HgCdTe films grown by molecular beam epitaxy on Si substrates*, Semicond. Sci. Technol., 2012, vol. 27, no. 3, art. no. 035001.
- [83] I.I. Izhnin, K.D. Mynbaev, M.V. Yakushev, A.I. Izhnin, E.I. Fitsych, N.L. Bazhenov, A.V. Shilyaev, G.V. Savitskii, R. Jakiela, A.V. Sorochkin, V.S. Varavin, S.A. Dvoretzky, *Electrical and Optical Properties of CdHgTe Films Grown by Molecular-Beam Epitaxy on Silicon Substrates*, Semiconductors, 2012, vol. 46, no. 10, pp. 1341–1345.
- [84] I.I. Izhnin, A.I. Izhnin, H.V. Savytskyy, O.I. Fitsych, N.N. Mikhailov, V.S. Varavin, S.A. Dvoretzky, Yu.G. Sidorov, K.D. Mynbaev, *Defects in HgCdTe grown by molecular beam epitaxy on GaAs substrates*, Opto-Electron. Review, 2012, vol. 20, no. 4, pp. 375–378.
- [85] S.A. Dvoretzky, M.F. Stupak, N.N. Mikhailov, V.S. Varavin, V.G. Remesnik, S.N. Makarov, A.G. Elesin, A.G. Verkhoglyad, *New recombination centers in MBE MCT films on GaAs substrates*, Fizika Tvyordogo Tela, 2023, vol. 65, no. 1, pp. 56–62 (in Russian).
- [86] J.P. Zanatta, F. Noël, P. Ballet, N. Hdadach, A. Million, G. Destefanis, E. Mottin, C. Kopp, E. Picard, E. Hadji, *HgCdTe Molecular Beam Epitaxy Material for Microcavity Light Emitters: Application to Gas Detection in the 2–6 μm Range*, J. Electron. Mater., 2003, vol. 32, no. 7, pp. 602–607.
- [87] E. Hadji, E. Picard, C. Roux, E. Molva, P. Ferret, *3.3-μm microcavity light emitter for gas detection*, Opt. Lett., 2000, vol. 25, no. 10, pp. 725–727.
- [88] K.D. Mynbaev, N.L. Bazhenov, A.V. Shilyaev, S.A. Dvoretzky, N.N. Mikhailov, M.V. Yakushev, V.G. Remesnik, V.S. Varavin, *High-temperature photoluminescence of CdHgTe solid solutions grown by molecular-beam epitaxy*, Tech. Phys., 2013, vol. 58, no. 10, pp. 1536–1539.
- [89] I.I. Izhnin, A.I. Izhnin, K.D. Mynbaev, N.L. Bazhenov, A.V. Shilyaev, N.N. Mikhailov, V.S. Varavin, S.A. Dvoretzky, O.I. Fitsych, A.V. Voitsekhovskiy, *Photoluminescence of HgCdTe nanostructures grown by molecular beam epitaxy on GaAs*, Opto-Electron. Review, 2013, vol. 21, no. 4, pp. 390–394.
- [90] I.I. Izhnin, A.I. Izhnin, K.D. Mynbaev, N.L. Bazhenov, E.I. Fitsych, M.V. Yakushev, N.N. Mikhailov, V.S. Varavin, S.A. Dvoretzky, *Photoluminescence of CdHgTe solid solutions subjected to low-energy ion treatment*, Semiconductors, 2014, vol. 48, no. 2, pp. 195–198.
- [91] K.D. Mynbaev, N.L. Bazhenov, M.V. Yakushev, D.V. Marin, V.S. Varavin, Yu.G. Sidorov, S.A. Dvoretzky, *Defects in heteroepitaxial CdHgTe/Si layers and their behavior under conditions of implanted p<sup>+</sup>-n photodiode structure formation*, Tech. Phys. Lett., 2014, vol. 40, no. 8, pp. 708–711.
- [92] S.V. Zablotsky, K.D. Mynbaev, N.L. Bazhenov, M.V. Yakushev, D.V. Marin, V.S. Varavin, S.A. Dvoretzky, *Acceptor states and carrier lifetime in heteroepitaxial HgCdTe*

- on-Si for mid-infrared photodetectors*, J. Phys.: Conf. Ser., 2015, vol. 643, art. no. 012004.
- [93] K.D. Mynbaev, A.V. Shilyaev, N.L. Bazhenov, A.I. Izhnin, I.I. Izhnin, N.N. Mikhailov, V.S. Varavin, S.A. Dvoretzky, *Acceptor States in Heteroepitaxial CdHgTe Films Grown by Molecular-Beam Epitaxy*, Semiconductors, 2015, vol. 49, no. 3, pp. 367–372.
- [94] K.D. Mynbaev, S.V. Zablotsky, A.V. Shilyaev, N.L. Bazhenov, M.V. Yakushev, D.V. Marin, V.S. Varavin, S.A. Dvoretzky, *Defects in Mercury-Cadmium Telluride Heteroepitaxial Structures Grown by Molecular-Beam Epitaxy on Silicon Substrates*, Semiconductors, 2016, vol. 50, no. 2, pp. 208–211.
- [95] M.V. Yakushev, K.D. Mynbaev, N.L. Bazhenov, V.S. Varavin, N.N. Mikhailov, D.V. Marin, S.A. Dvoretzky, Yu.G. Sidorov, *Acceptor states in HgCdTe films grown by molecular-beam epitaxy on GaAs and Si substrates*, Phys. Status Solidi C, 2016, vol. 13, no. 7–9, pp. 469–472.
- [96] A.P. Kovchavtsev, A.A. Guzev, A.V. Tsarenko, Z.V. Panova, M.V. Yakushev, D.V. Marin, V.S. Varavin, V.V. Vasilyev, S.A. Dvoretzky, I.V. Sabinina, Yu.G. Sidorov, *The reverse current temperature dependences of SWIR CdHgTe “p-on-n” and “n-on-p” junctions*, Infr. Phys. Technol., 2015, vol. 73, pp. 312–315.
- [97] M.A. Kinch, F. Aqariden, D. Chandra, P.-K. Liao, H.F. Schaake, H.D. Shih, *Minority carrier lifetime in p-HgCdTe*, J. Electron. Mater., 2005, vol. 34, no. 6, pp. 880–884.
- [98] K.D. Mynbaev, N.L. Bazhenov, S.A. Dvoretzky, N.N. Mikhailov, V.S. Varavin, D.V. Marin, M.V. Yakushev, *Photoluminescence of Molecular Beam Epitaxy-Grown Mercury Cadmium Telluride: Comparison of HgCdTe/GaAs and HgCdTe/Si Technologies*, J. Electron. Mater., 2018, vol. 47, no. 8, pp. 4731–4736.
- [99] A.O. Timoshkov, N.L. Bazhenov, K.D. Mynbaev, V.S. Varavin, M.V. Yakushev, N.N. Mikhailov, S.A. Dvoretzky, *Photoluminescence of Hg<sub>0.5</sub>Cd<sub>0.5</sub>Te structures grown with molecular-beam epitaxy*, Mater. Phys. Mech., 2017, vol. 32, no. 1, pp. 88–93.
- [100] N.D. Akhavan, G.A. Umana-Membreno, R. Gu, J. Antoszewski, L. Faraone, *Design Principles for High QE HgCdTe Infrared Photodetectors for eSWIR Applications*, J. Electron. Mater., 2022, vol. 51, no. 9, pp. 4742–4751.
- [101] M. Zhu, I. Prighozhin, P. Mitra, R. Scritchfield, C. Schaake, J. Martin, J.H. Park, F. Aqariden, E. Bellotti, *Dark Current and Gain Modeling of Mid-Wave and Short-Wave Infrared Compositionally Graded HgCdTe Avalanche Photodiodes*, IEEE Trans. Electron. Dev., 2022, vol. 69, no. 9, pp. 4962–4969.
- [102] N.L. Bazhenov, B.L. Gelmont, V.I. Ivanov-Omskii, A.I. Izhnin, V.A. Smirnov, *Photoluminescence of Cd<sub>0.4</sub>Hg<sub>0.6</sub>Te Solid-Solutions*, Sov. Phys. – Semiconductors, 1990, vol. 24, no. 1, pp. 56–59.
- [103] V.I. Ivanov-Omskii, K.D. Mynbaev, I.N. Trapeznikova, D.A. Andryushchenko, N.L. Bazhenov, N.N. Mikhailov, V.S. Varavin, V.G. Remesnik, S.A. Dvoretzky, M.V. Yakushev, *An Optical Study of Disorder in Cadmium Mercury Telluride Solid Solutions*, Tech. Phys. Lett., 2019, vol. 45, no. 6, pp. 553–556.
- [104] D.A. Andryushchenko, I.N. Trapeznikova, N.L. Bazhenov, M.A. Yagovkina, K.D. Mynbaev, V.G. Remesnik, V.S. Varavin, *Strong Disorder in HgCdTe Studied with Optical Methods and X-Ray Diffraction*, J. Phys.: Conf. Ser., 2019, vol. 1400, art. no. 066038.
- [105] Yu.G. Sidorov, A.P. Anciferov, V.S. Varavin, S.A. Dvoretzky, N.N. Mikhailov, M.V. Yakushev, I.V. Sabinina, V.G. Remesnik, D.G. Ikusov, I.N. Uzhakov, G.Yu. Sidorov, V.D. Kuzmin, S.V. Rihlicky, V.A. Shvets, A.S. Mardezov, E.V. Spesivcev, A.K. Gutakovskii, A.V. Latyshev, *Molecular Beam Epitaxy of Cd<sub>x</sub>Hg<sub>1-x</sub>Te*, Chapter 12, in: *Advances in Semiconductor Nanostructures: Growth, Characterization, Properties and Applications*, ed. by A.V. Latyshev, A.V. Dvurechenskii, A.L. Aseev, Elsevier, Amsterdam, 2017, pp. 297–323.
- [106] D.A. Andryushchenko, N.L. Bazhenov, K.D. Mynbaev, N.N. Mikhailov, V.G. Remesnik, *Optical studies of wide-bandgap HgCdTe material used in potential-and quantum-well structures*, J. Phys.: Conf. Ser., 2020, vol. 1482, art. no. 012002.
- [107] K.D. Mynbaev, A.M. Smirnov, N.L. Bazhenov, N.N. Mikhailov, V.G. Remesnik, M.V. Yakushev, *Optical Studies of Molecular-Beam Epitaxy-Grown Hg<sub>1-x</sub>Cd<sub>x</sub>Te with x = 0.7–0.8*, J. Electron. Mater., 2020, vol. 49, no. 8, pp. 4642–4646.
- [108] K.D. Mynbaev, N.L. Bazhenov, A.M. Smirnov, N.N. Mikhailov, V.G. Remesnik, M.V. Yakushev, *Optical and Structural Properties of HgCdTe Solid Solutions with a High CdTe Content*, Semiconductors, 2020, vol. 54, no. 12, pp. 1561–1566.
- [109] V.A. Shvets, N.N. Mikhailov, D.G. Ikusov, I.N. Uzhakov, S.A. Dvoretzky, *Determining the Compositional Profile of HgTe/Cd<sub>x</sub>Hg<sub>1-x</sub>Te Quantum Wells by Single-Wavelength Ellipsometry*, Opt. Spectrosc., 2019, vol. 127, no. 2, pp. 340–346.
- [110] C.R. Becker, T.N. Casselman, C.H. Grein, S. Sivanathan, *Molecular Beam Epitaxy of HgCdTe Materials and Detectors*, Chapter 6.04, in: *Comprehensive Semiconductor Science and Technology*, vol. 6, ed. by P. Bhattacharya, R. Fornari, H. Kamimura, Elsevier, Amsterdam, 2011, pp. 128–159.
- [111] D.A. Andryushchenko, M.S. Ruzhevich, A.M. Smirnov, N.L. Bazhenov, K.D. Mynbaev, *Optical and structural studies of Hg<sub>0.7</sub>Cd<sub>0.3</sub>Te samples grown by various methods*, J. Phys.: Conf. Ser., 2021, vol. 2103, art. no. 012148.
- [112] D.A. Andryushchenko, M.S. Ruzhevich, A.M. Smirnov, N.L. Bazhenov, K.D. Mynbaev, V.G. Remesnik, *Optical and Structural Properties of Hg<sub>0.7</sub>Cd<sub>0.3</sub>Te Epitaxial Films*, Semiconductors, 2022, vol. 56, no. 13, pp. 2063–2067.
- [113] W. Gawron, J. Sobieski, T. Manyk, M. Kopytko, P. Madejczyk, J. Rutkowski, *MOCVD Grown HgCdTe Heterostructures for Medium Wave Infrared Detectors*, Coatings, 2021, vol. 11, no. 5, art. no. 611.
- [114] A. Rogalski, *Scaling infrared detectors — status and outlook*, Rep. Prog. Phys., 2022, vol. 85, no. 12, art. no. 126501.

УДК 535–15

## Фотолюминесценция теллуридов кадмия-ртути – историческая ретроспектива. Часть II: 2004–2022

М.С. Ружевич<sup>1</sup>, К.Д. Мынбаев<sup>1,2</sup>

<sup>1</sup> Институт перспективных систем передачи данных, Университет ИТМО, Кронверкский пр., 49, лит. А, Санкт-Петербург 197101, Россия

<sup>2</sup> Отделение физики твердого тела, ФТИ им. А.Ф. Иоффе, Политехническая ул., 26, лит. А, Санкт-Петербург 194021, Россия

**Аннотация.** Настоящая статья является второй частью обзора, в котором рассматривается историческая ретроспектива исследований фотолюминесценции в теллуридах кадмия-ртути (HgCdTe), одном из важнейших материалов инфракрасной фотоэлектроники. Во второй части обзора рассматриваются результаты исследований, выполненных в 2004–2022 гг. Эти исследования проводились в основном на пленках, выращенных методом молекулярно-лучевой эпитаксии, и были сосредоточены на изучении дефектов, особенно тех, которые формируются при легировании HgCdTe материала в р-тип проводимости вакансиями ртути или атомами мышьяка. Предметами исследований также были однородность состава и флуктуации состава твердого раствора в HgCdTe.

*Ключевые слова:* теллуриды кадмия-ртути; люминесценция; дефекты; флуктуации состава твердого раствора